Journal of Medicinal Chemistry

Article

pubs.acs.org/jmc

Garcinia Xanthones as Orally Active Antitumor Agents

Xiaojin Zhang,[†,‡,∥] Xiang Li,[‡] Haopeng Sun,*[,‡,§] Xiaojian Wang,[#] Li Zhao,[⊥] Yuan Gao,[⊥] Xiaorong Liu,[§] Shenglie Zhang,[‡,§] Yanyan Wang,[‡,§] Yingrui Yang,[‡,§] Su Zeng,[▽] Qinglong Guo,*[,⊥] and Qidong You*[,†,‡]

[†]State Key Laboratory of Natural Medicines, [‡]Jiangsu Key Laboratory of Drug Design and Optimization, [§]Department of Medicinal Chemistry, School of Pharmacy, [∥]Department of Organic Chemistry, School of Science, and [⊥]Jiangsu Key Laboratory of Carcinogenesis and Intervention, China Pharmaceutical University, Nanjing, 210009, China

[#]Institute of Materia Medica, Chinese Academy of Medical Science and Peking Union Medical College, Peking, 10005, China

[▽]Department of Pharmaceutical Analysis and Drug Metabolism, College of Pharmaceutical Sciences, Zhejiang University, Hangzhou, 310058, China

Supporting Information

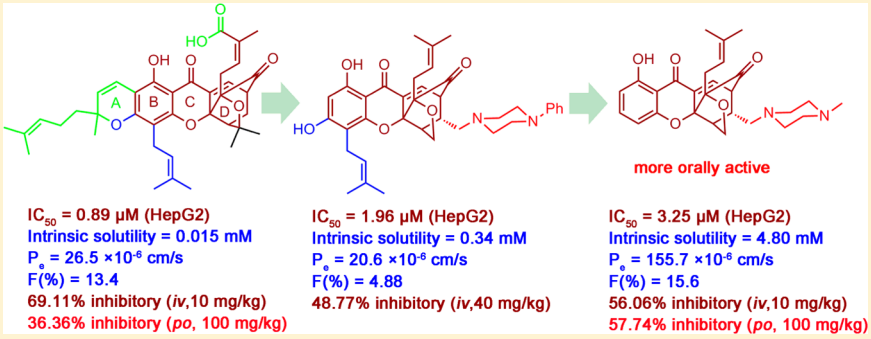

ABSTRACT: Using a newly developed strategy whose key step is the regioselective propargylation of hydroxyxanthone substrates, 99 structurally diverse *Garcinia* natural-product-like xanthones based on gambogic acid were designed and synthesized and their in vitro antitumor activity was evaluated. A set of 40 related compounds was chosen for determination of their physicochemical properties including polar surface area, log $D_{7.4}$, aqueous solubility, and permeability at pH 7.4. In the light of the in vitro antitumor activity and the physicochemical properties, two compounds were advanced into in vivo efficacy experiments. The antitumor activity of compound **112**, administered po, showed more potent in vivo oral antitumor activity than gambogic acid.

INTRODUCTION

Natural products (NP) are a unique source of diverse bioactive lead compounds for drug discovery. More than 50% of the drugs developed in the pharmaceutical industry over the past 30 years are NPs or inspired by NP structures.[1,2] In the case of anticancer drugs, the proportion is even higher; 74.8% of the anticancer drugs approved worldwide between 1940 and December 2010 owe their origins to NPs.[1] The evolutionary selection processes has resulted in complex bioactive NPs with diverse structures that are optimized to interact with various biological systems. Due to their coevolution with the target sites in biological systems, the quality of leads arising from NP scaffolds is considered to be superior and often more biologically friendly.[3] NP scaffolds are in fact privileged templates for rapid identification of promising new chemical entities for therapeutic applications.

The gambogin resin secreted by the *Garcinia* genus of tropical plants has been used as folk medicine for centuries in Southeast Asia.[4] Efforts to identify the bioactive constituents of gambogin resin have revealed a growing family of natural products known as "caged xanthones" based on their unique 4-oxa-tricyclo[4.3.1.$0^{3,7}$]decan-2-one scaffold with a common xanthone backbone.[5] This motif is further elaborated by substitutions on the aromatic residue and peripheral oxidations to produce a variety of structurally diverse caged *Garcinia* xanthones shown in Figure 1, including gambogic acid (GA, **1**),[6,7] gambogellic acid (**2**),[8] desoxymorellin (**3**),[9] gaudichaudione A (**4**),[10] gaudichaudione G (**5**),[10] and isobractatin (**6**).[11] Among these, **1** is the most prominent and representative example. Preclinical investigation identified **1** as a potent antitumor agent that inhibits the growth of a broad panel of cancer cell lines both in vitro and in vivo.[12−15] Biological studies revealed that the antitumor efficacy of **1** arises through multiple mechanisms involving apoptosis induction,[16,17] cell cycle regulation,[18] angiogenesis inhibition,[19,20] tumor cell adhesion inhibition, and metastasis prevention.[21] Biomolecular targets of GA that have been reported include the bcl-2 family,[22] p53/mdm2 complex,[16] cytosolic thioredoxins,[23] topoisomerase II,[24] survivin,[25] transferring receptor,[26,27] heat

Received: October 29, 2012
Published: November 20, 2012

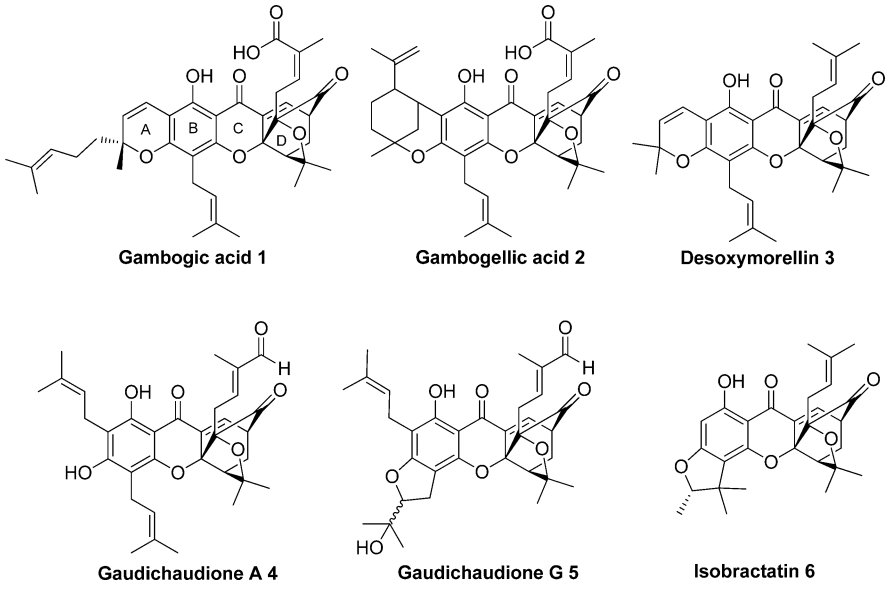

Figure 1. Caged *Garcinia* xanthones with conservative D caged ring and structurally diverse AB-ring.

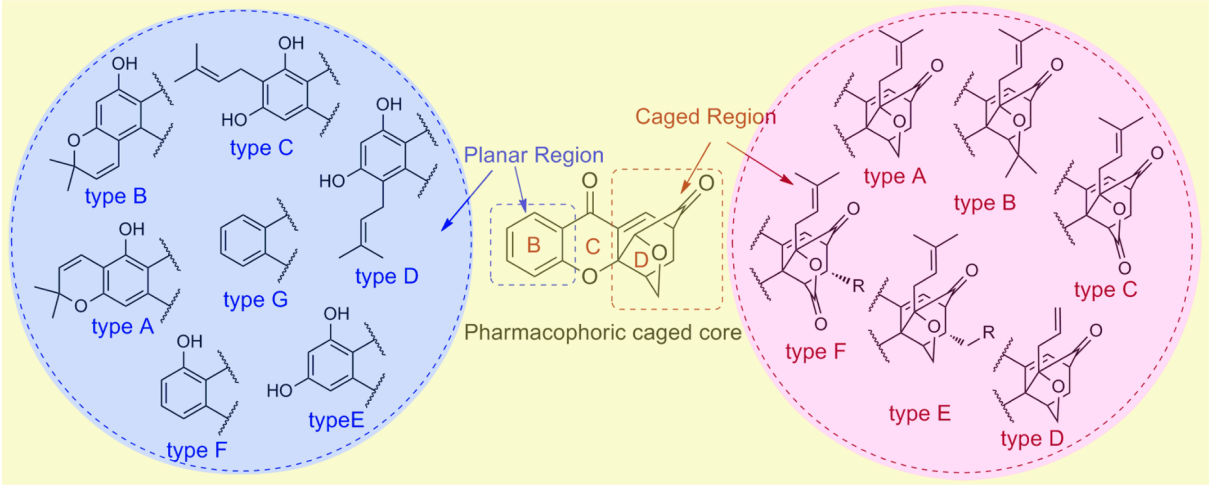

Figure 2. Designed *Garcinia* natural-product-like caged xanthones with a pharmacophoric caged core.

shock protein 90,[28] stathmin,[29] and IκBα kinase-β protein,[30,31] which could explain some aspects of the mechanism of action. In addition, GA showed minimal toxicity to normal cells and has a potentially useful therapeutic window in cancer treatment.[14,15]

Unfortunately, some perceived disadvantages of GA limit its clinical application. These include limited natural sources and complexities associated with its isolation in approximately 5% yield from the gamboges resin,[6,32] difficulties in the total synthesis,[33] very low aqueous solubility (about 0.01 mg/mL),[34] and considerable loss of potency when administered orally. Although several simpler analogues such as cluvenone (**34**) and 1-hydroxycluvenone (**33**) have been synthesized and reported to possess the cytotoxicity exhibited by GA against some cancer cell lines,[35−38] these compounds still lacked the druglike properties optimal for further preclinical development. Preliminary SAR studies indicated that the α,β-unsaturated ketone moiety of CD caged region[13] in GA as well as its BC planar region are both essential for the antitumor activity of GA,[31,37−39] and the peripheral moieties are suitable as sites for diverse modification.[13,32,40−44] In view of the limited exploration that has been reported of the planar ring B and the caged ring D in simplified *Garcinia* analogues, we were prompted to examine the *Garcinia* natural-product-like xanthones shown in Figure 2. These compounds have diverse structures based on the pharmacophoric caged core associated with antitumor efficacy, and we conducted both detailed structure−activity relationship (SAR) and structure−property relationship (SPR) studies. Our synthetic strategy was mainly based upon the regioselective propargylation of diverse hydroxyxanthone substrates followed by a Claisen/Diels−Alder cascade reaction to generate different planar B-rings and caged D-rings. All the *Garcinia* natural-product-like caged xanthones have been tested in vitro for antitumor activities against the human hepatocellular carcinoma HepG2 cell line, the human lung carcinoma A549 cell line, and the human glioblastoma U251 cell line. Forty representative compounds have been evaluated for intrinsic aqueous solubility, polar surface area (PSA), log *D*, and permeability at pH 7.4 to identify the compounds with potential to be advanced into in vivo efficacy experiments. The compounds with effective in vivo antitumor activity have been evaluated for their in vivo

dx.doi.org/10.1021/jm301593r | J. Med. Chem. 2013, 56, 276−292

Scheme 1. Substrates Tested in the Propargylation Reaction and Their Probable Products[a]

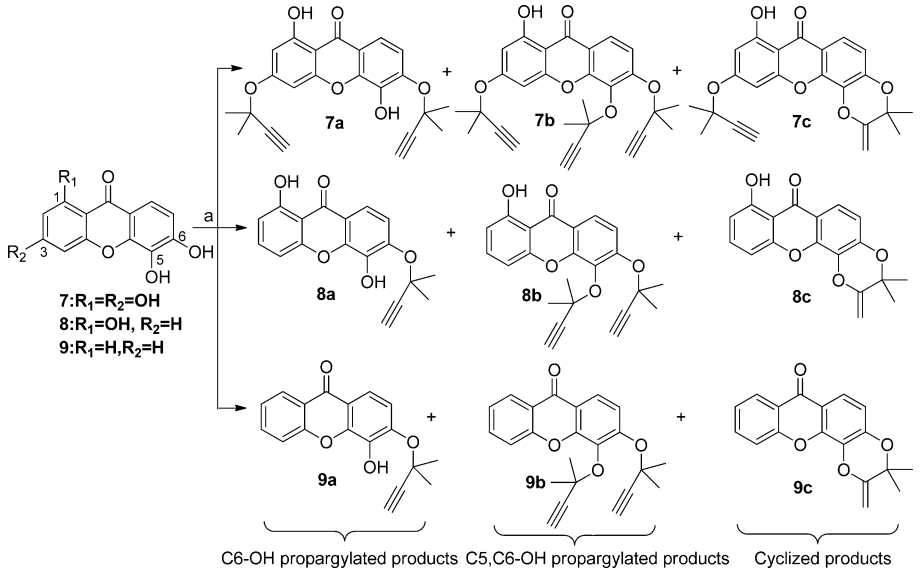

[a]Reagents and conditions: (a) 3-chloro-3-methylbut-1-yne (5 equiv for substrate **7**, 2.5 equiv for substrates **8** and **9**), K_2CO_3 (3.3 equiv for substrate **7**, 2.2 equiv for substrates **8** and **9**), KI, 10 mol % CuI. For detailed reaction conditions see Table 1.

Table 1. Regioselectivity in Propargylation of Hydroxyxanthone Substrates

entry	substrate	solvent	T (°C)	t (h)	products (% yield)			substrate recovery (%)
1	**7**	Me_2CO	reflux	6	**7a** (0)	**7b** (25)	**7c** (61)	0
2	**7**	Me_2CO	reflux	2	**7a** (12)	**7b** (10)	**7c** (41)	28
3	**7**	Me_2CO	35	6	**7a** (15)	**7b** (0)	**7c** (27)	50
4	**7**	Me_2CO	20	6	**7a** (0)	**7b** (0)	**7c** (0)	98
5	**7**	CH_3CN	20	6	**7a** (7)	**7b** (0)	**7c** (1)	82
6	**7**	CH_3CN	35	6	**7a** (22)	**7b** (0)	**7c** (13)	60
7	**7**	CH_3CN	50	2	**7a** (10)	**7b** (7)	**7c** (47)	28
8	**7**	THF	20	6	**7a** (0)	**7b** (0)	**7c** (0)	99
9	**7**	THF	35	6	**7a** (2)	**7b** (0)	**7c** (0)	95
10	**7**	CH_3CH/THF (4:1)	35	6	**7a** (35)	**7b** (0)	**7c** (9)	50
11	**7**	CH_3CH/THF (2:1)	35	6	**7a** (41)	**7b** (0)	**7c** (8)	43
12	**7**	CH_3CH/THF (1:1)	35	6	**7a** (10)	**7b** (0)	**7c** (3)	82
13	**8**	Me_2CO	reflux	6	**8a** (0)	**8b** (0)	**8c** (88)	0
14	**8**	CH_3CN/THF (2:1)	35	6	**8a** (42)	**8b** (0)	**8c** (2)	50
15	**9**	Me_2CO	reflux	6	**9a** (0)	**9b** (80)	**9c** (11)	0
16	**9**	CH_3CN/THF (2:1)	35	6	**9a** (33)	**9b** (0)	**9c** (3)	52

pharmacokinetic parameters to determine which of them are potentially orally active. In this paper, we report the preparation and thorough examination of a library of 99 *Garcinia* natural-product-like caged xanthones and the discovery of novel *Garcinia* caged xanthones as orally active antitumor agents.

RESULTS AND DISCUSSION

Synthetic Chemistry. The unique 4-oxatricyclo[4.3.1.$0^{3,7}$]-decan-2-one caged structure of these *Garcinia* natural-product-like xanthones can be synthesized using the well-established Claisen rearrangement/intramolecular Diels–Alder cascade reaction,[45−51] and the structural diversity of the target *Garcinia* caged xanthone analogues depends on that of the precursors in the rearrangement. However, previous synthetic approaches were limited in practice to provide two main chemical types of rearrangement precursors: bis-allyl and bis(2-methylbut-3-enyl) compounds.[33] In the present study, a new synthetic strategy was developed to generate structural diversity in both the caged and planar regions to obtain detailed SAR and SPR data and to improve the druglike properties. This strategy was based on the regioselective propargylation of the OH group at C6 of the 5,6-dihydroxyxanthone substrates, leaving the C5-OH group free for introduction of various allyl substituents to form diverse rearrangement precursors producing diverse target caged structures.

The 5,6-dihydroxyxanthones **7**–**9** (Scheme 1) were the starting points for the propargylation reactions, which could be conveniently effected according to our previously reported methods.[38,48] Using of 3-chloro-3-methylbut-1-yne in the presence of KI and K_2CO_3 and CuI as catalyst was essential for this alkylation.[47] Refluxing substrate **7** in Me_2CO for 6 h led to alkylation, providing cyclized product **7c** and the C5, C6-OH propargylated product **7b** but none of the desired C6-OH propargylated product **7a** (Table 1, entry 1). Although no **7a** was isolated at the end of the reaction, the formation of **7c** suggested that **7a** might arise during the reaction because **7c** probably formed from **7a** under CuI catalysis. With lower temperatures (35 °C) (Table 1, entry 2) or shorter reaction

dx.doi.org/10.1021/jm301593r | J. Med. Chem. 2013, 56, 276−292

Scheme 2. Synthesis of Caged Xanthone Analogues 18−23 Missing One *gem*-Dimethyl Group in the Caged Region[a]

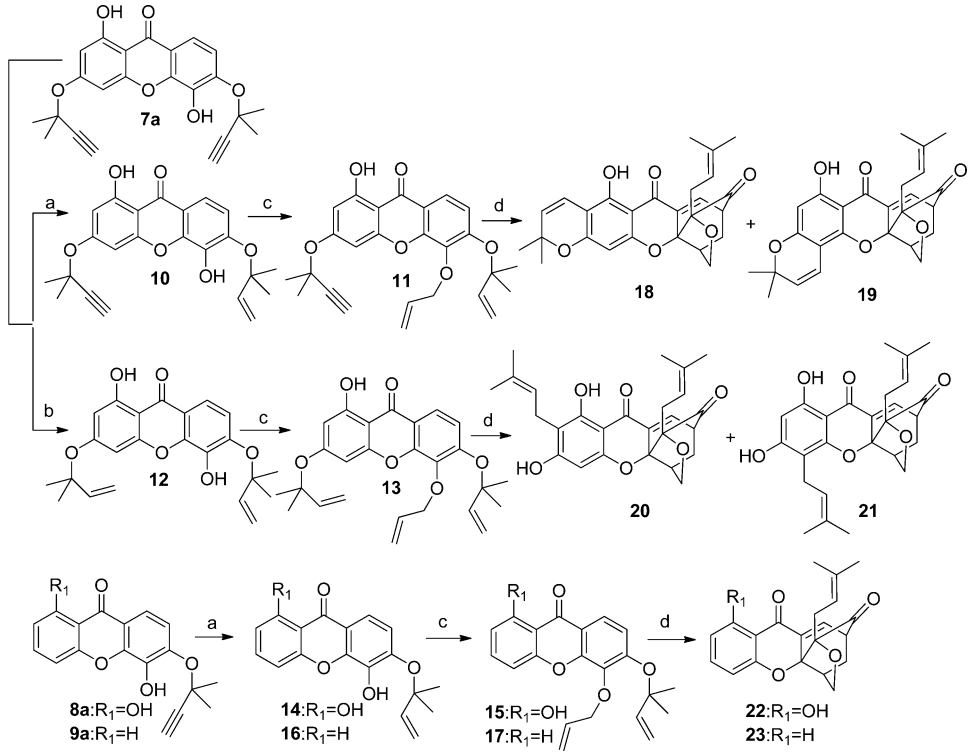

[a]Reagents and conditions: (a) H_2, Pd/$BaSO_4$, EtOH, 25 °C, 20 min, 82−89%; (b) H_2, Pd/$BaSO_4$, EtOH, 25 °C, 40 min, 90%; (c) allyl bromide, K_2CO_3, Me_2CO, 35 °C, 4 h, 79−87%; (d) DMF, 120 °C, 2 h, 71−86%.

Scheme 3. Synthesis of Caged Xanthone Analogues 28−34 with Two *gem*-Dimethyl Groups in the Caged Region[a]

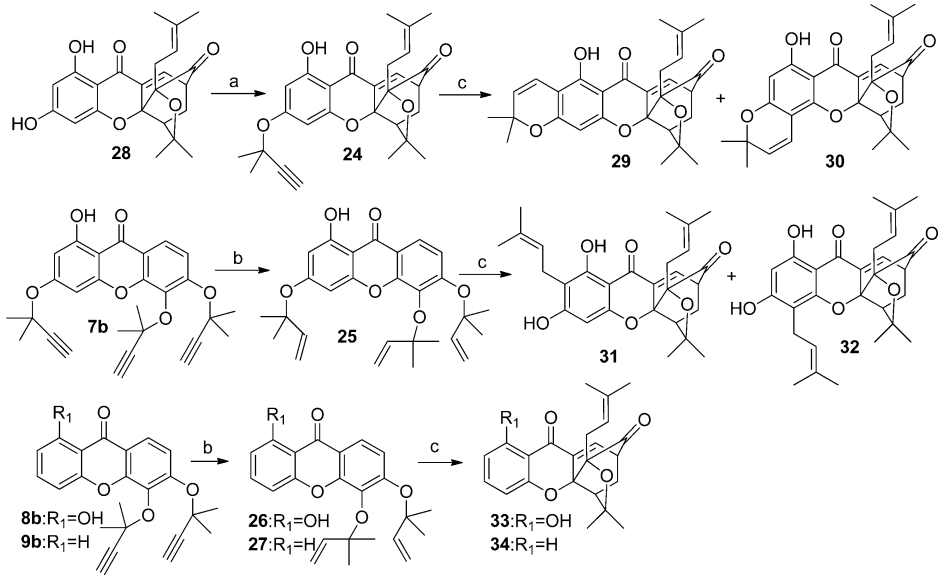

[a]Reagents and conditions: (a) 3-chloro-3-methylbut-1-yne, K_2CO_3, KI, 10% CuI, Me_2CO, reflux, 30 min, 85%; (b) H_2, Pd/$BaSO_4$, EtOH, 25 °C, 40 min, 80−89%; (c) DMF, 120 °C, 2 h, 57−82%.

times (Table 1, entry 3), relatively low yields of the C6-OH propargylated product **7a** were obtained, but it was not produced by the reaction carried out at 20 °C in Me_2CO (Table 1, entry 4). Different solvents such as CH_3CN, THF, and their mixtures were also evaluated in order to improve the yield and selectivity of **7a** (Table 1, entries 5−12), and it was found that in CH_3CN, **7a** was formed even at 20 °C (Table 1, entry 5). A significant proportion of **7** was not converted to **7a** in this reaction as a result of its low solubility in CH_3CN at such relatively low reaction temperatures (Table 1, entries 5, 6), and increases in reaction temperature led to an increased ratio of the cyclized product **7c**. Meanwhile, the solvent THF, in which the solubility of **7** was enhanced, was found to seriously hinder the propargylation process (Table 1, entries 8, 9). Subsequently, use of CH_3CN/THF mixtures (v:v = 2:1) as solvent was found to give an improved yield (41%) of **7a** with

dx.doi.org/10.1021/jm301593r | J. Med. Chem. 2013, 56, 276−292

acceptable regioselectivity between C6-OH and C5-OH groups (Table 1, entry 11). In a similar manner, using CH_3CN/THF as solvent at 35 °C, substrates **8** and **9** selectively provided the C6-OH monopropargylated products **8a** and **9a**, respectively (Table 1, entries 14, 16), but no C6-OH monopropargylated products were observed when refluxing **7**, **8**, or **9** in Me_2CO (Table 1, entries 13, 15). Despite the moderate C6-OH propargylation yields (33−42%) and the recovery of reactants, this strategy offered the most expedient selective route to the C6-OH propargylated products **7a**−**9a**, the key intermediates to generate the diverse target *Garcinia* caged xanthones.

Next, a set of caged xanthones varying in both the planar and caged regions was synthesized to probe the substituent groups around the pharmacophoric caged core (Schemes 2−4). With

Scheme 4. Synthesis of Caged Xanthone Analogues 36 Missing the Two *gem*-Dimethyl Groups in the Caged Region[a]

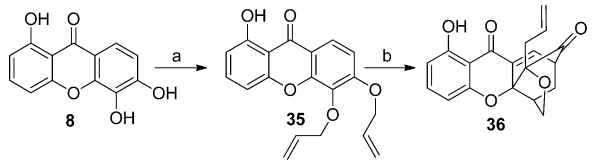

[a]Reagents and conditions: (a) allyl bromide, K_2CO_3, Me_2CO, 35 °C, 4 h, 95%; (b) decalin, 180 °C, 3 h, 51%.

the C6-OH propargylated xanthones **7a**−**9a** in hand, caged xanthone analogues **18**−**23** missing one *gem*-dimethyl group in the caged region were synthesized through routes similar to that in Scheme 2. Regioselective monohydrogenation of the acetylenic moiety at C6 in **7a** in the presence of Lindlar catalyst provided the corresponding olefin **10** by curtailing the reaction time to 20 min. With further prolongation of the reaction time to 40 min, both the C5 and C6 acetylenic moieties in **7a** were reduced to the olefin **12**. Subsequent alkylation of **10** and **12** in the presence of allyl bromide and K_2CO_3 gave rise to **11** and **13**, respectively. Drawing on previous experience with related structures[50] we heated **11** in DMF at 120 °C utilizing the Claisen/Diels−Alder/Claisen reaction and obtained the caged xanthones **18** and **19** as isomers with a pyran ring merged into planar region, that at the C2 and C4 positions, respectively (Scheme 2). Meanwhile, in the case of **13**, caged xanthones **20** and **21** were formed as isomers with a prenyl group at the C2 and C4 positions, respectively (Scheme 2). In a similar manner, intermediates **8a** and **9a** underwent Lindlar reduction and allylation followed by Claisen/Diels−Alder cascade reaction to form, respectively, the caged xanthones **22** and **23** with a simple planar region (Scheme 2). On the basis of the caged compound **28** previously developed in our laboratory,[49] the caged xanthone analogues **29** and **30**, with a pyran ring in the planar region and both the *gem*-dimethyl groups in the caged region, were obtained by propargylation of the C3-OH group using 3-chloro-3-methylbut-1-yne followed by Claisen rearrangement cyclization (Scheme 3). Caged xanthones **31** and **32** (forbesione) were prepared as shown in Scheme 3 according to published reactions,[31,47] and compounds **33** (cluvenone) and **34** (1-hydroxycluvenone) were prepared according to our previously reported procedure (Scheme 3).[38] In addition, caged xanthone **36**, from which the two *gem*-dimethyl group in the caged region are absent, was prepared from the xanthone **8** by diallylation to form **35** and, subsequently, Claisen/Diels−Alder reaction in decalin at 180 °C (Scheme 4).

Subsequently, a number of D-ring-modified caged xanthones (**46**−**130**) were designed to probe the caged region and to determine the optimal substitution for antitumor activity as well as druglike properties (Scheme 5). Compound **10** was allylated with (*E*)-1,4-dibromobut-2-ene in the presence of K_2CO_3 in Me_2CO, generating the intermediate **37**, derivatization of which with various aliphatic or aromatic amines, alcohols, or acids in the presence of K_2CO_3 in DMF led to the precursor **38**, which underwent the Claisen/Diels−Alder reaction to provide the caged xanthones **46**−**52** and **53**−**59** as isomer pairs, with a pyran ring in the planar region and a modified caged region (Scheme 5). Similarly, D-ring-modified caged xanthones **60**−**81** and **82**−**103** were obtained from compound **12**, which possessed a prenyl group in its planar region (Scheme 5). Treatment of **12** with various acrylic acids in the presence of 1-ethyl-3-(3-dimethylaminopropyl)carbodiimide hydrochloride (EDC·HCl) and 4-dimethylaminopyridine (DMAP) in DCM led to the ethers **41a**−**d**. Heating precursors **41a**−**d** in DMF at 120 °C produced the caged xanthones **104**−**107** with a carbonyl group in the caged region, by replacing the *gem*-dimethyl group and a C4 substituted prenyl group in the planar region (Scheme 5). In this case, hardly any of the C2 prenylated isomer was isolated. Furthermore, by use of compounds **14** and **16** as synthetic entries instead of **12**, the D-ring-modified caged xanthones **108**−**130** with a simple planar region were similarly prepared as a single isomer (Scheme 5).

Antiproliferative Activities. The antiproliferative activity of **1** and the 99 synthetic *Garcinia* natural-product-like caged xanthones were assessed with the tetrazolium-based MTT assay using the human hepatocellular carcinoma HepG2 cell line, the human lung carcinoma A549 cell line, or the human glioblastoma U251 cell line. Cancer cells were treated with increasing concentrations of the compounds for 24 h, and then the cell viability was evaluated through measurements of mitochondrial dehydrogenase activity. The antiproliferative activities, expressed as IC_{50} values, are summarized in Tables 2−6. Compound **1** was used as positive control for the in vitro assay and exhibited IC_{50} values of 0.89, 1.10, and 2.56 μM against HepG2, A549, and U251 cells, respectively. In general, most of the caged xanthones showed potent antiproliferative activities against HepG2 and A549 cells, with IC_{50} values at low micromolar levels. All the compounds tested were found to be less sensitive to U251 cells than to HepG2 and A549 cells. Among the 99 synthetic caged xanthones, compound **33** showed the most potent inhibitory activities in vitro against HepG2 and A549 cells, with an IC_{50} value of 0.81 and 0.70 μM, respectively, while compound **78** was the most cytotoxic against U251 cells, with an IC_{50} value of 6.56 μM.

Structure−Activity Relationship Studies. First, a set of caged xanthones (Table 2) varying in both the planar region (seven structural types) and caged region (four structural types) was designed to gain an understanding of the SAR around the pharmacophoric caged core and especially to explore the optimal structure of the caged region for antitumor activity. As shown in Table 2, all the compounds seemed to be more active toward HepG2 and A549 cells but less active or even not active toward U251 cells at similar concentrations. In the cases of HepG2 and A549 cells, generally, compounds with type A (containing two *gem*-dimethyl groups) and type B (containing one *gem*-dimethyl group) caged regions were found

dx.doi.org/10.1021/jm301593r | J. Med. Chem. 2013, 56, 276−292

Scheme 5. Synthesis of D-Ring-Modified Caged Xanthone Analogues 46−130 with Diverse Planar Region[a]

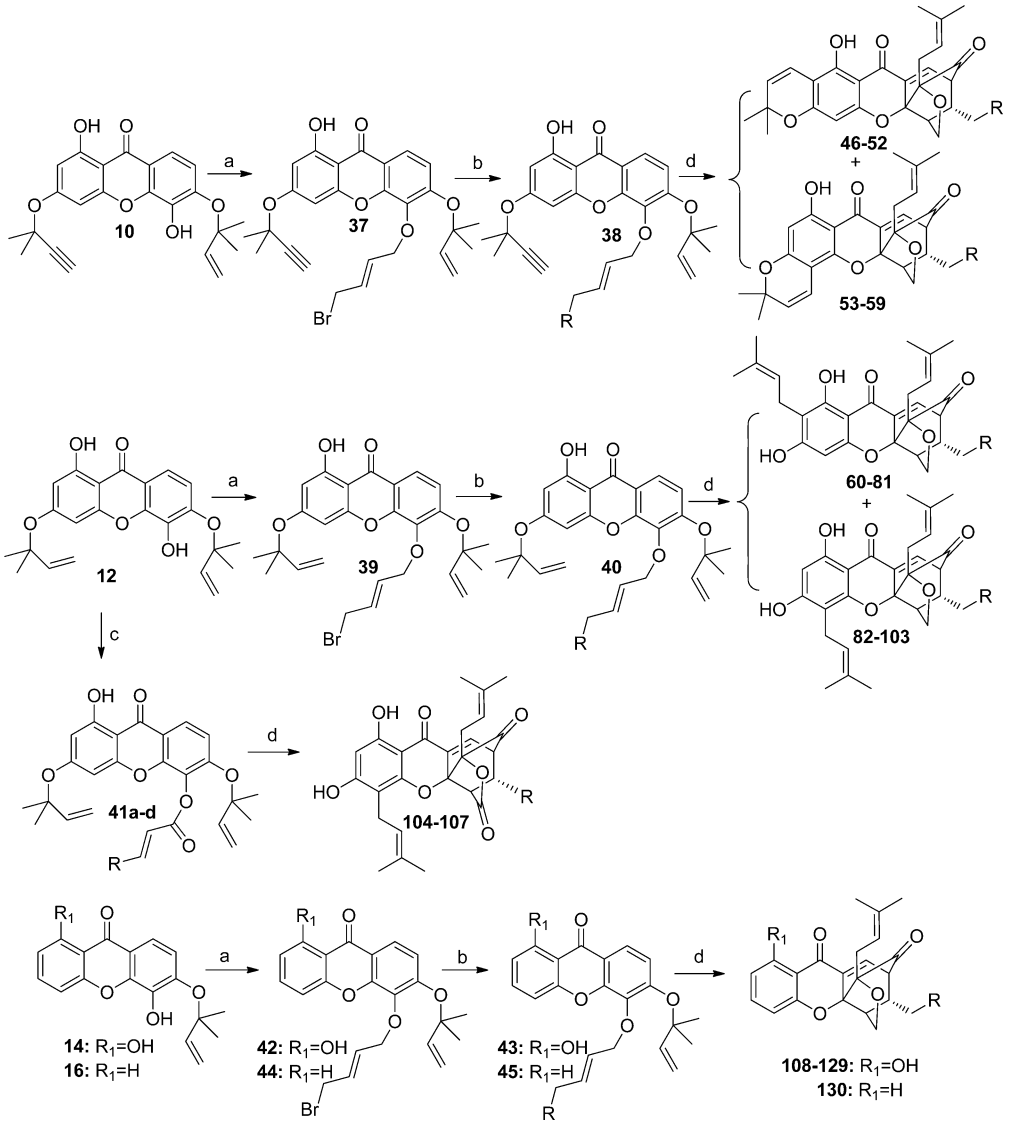

[a]Reagents and conditions: (a) (*E*)-1,4-dibromobut-2-ene, K_2CO_3, Me_2CO, 35 °C, 4 h, 74−77%; (b) different amide or alcohol or acid, K_2CO_3, DMF, 35 °C, 1 h, 99−100%; (c) substituted acrylic acid, EDC·HCl, DMAP, DCM, 25 °C, 2 h, 71−80%; (d) DMF, 120 °C, 2 h, 24−32% for **46−52**, 35−43% for **53−59**, 20−32% for **60−81**, 30−44% for **82−103**, 31−37% for **104−107**, and 51−70% for **108−130**. For the detailed R groups of compounds **46−130**, see Tables 3−6.

to be more active than that with type C (containing one *gem*-dimethyl group and one carbonyl group) or type D caged structures (missing two *gem*-dimethyl groups). For instance, compounds **22** and **33** possessed a low micromolar activity (0.70−3.79 μM) against HepG2 and A549 cells and were much more potent than compound **36**, which contains the same planar region. Similarly, compared with compounds **21** and **32**, compound **104**, with a carbonyl group in the caged region, was about 10−20-fold less active against A549 cells and inactive at 100 μM against HepG2 and U251 cells. Meanwhile, compounds **18−21** with type A caged structure displayed antitumor activity similar to that of the corresponding compounds **29−32** with type B caged moiety that lacked a *gem*-dimethyl group. The planar region with diverse structures including types A−G was found to be tolerated, whereas type G without any substituents contributed the least to their antitumor activity. Compound **22** for example, bearing a C1 hydroxyl group on the B-ring had IC_{50} values of 2.65 and 3.79 μM against HepG2 and A549 cells, respectively, while compounds **18−21**, containing the same caged structure as **22**, possessed similar IC_{50} values ranging from 2.04 to 8.43 μM. On the other hand, compound **23**, formed by the removal of the C1 hydroxyl group, when compared to **22**, was found to be almost 4−10-fold less active. Similar decreases in cytotoxicity were also observed between compounds **33** and **34**. These results suggest that (a) the *gem*-dimethyl group directly linked to the caged scaffold is not necessary for the bioactivity, (b) replacement of the *gem*-dimethyl group linked to the caged scaffold with a carbonyl group leads to substantial loss of activity, (c) the *gem*-dimethyl group of the prenyl moiety in the caged region contributes significantly to the antitumor activity, and (d) the prenylation and pyran fusion in the B-ring planar region are well-tolerated and the C1 hydroxyl group on B-ring benefits the cytotoxicity.

On the basis of the above SAR around the pharmacophoric caged core, a large set of D-ring-modified caged xanthones **46−**

dx.doi.org/10.1021/jm301593r | *J. Med. Chem.* 2013, 56, 276−292

Table 2. SAR of the Planar Region and *gem*-Dimethyl Group in the Caged Region

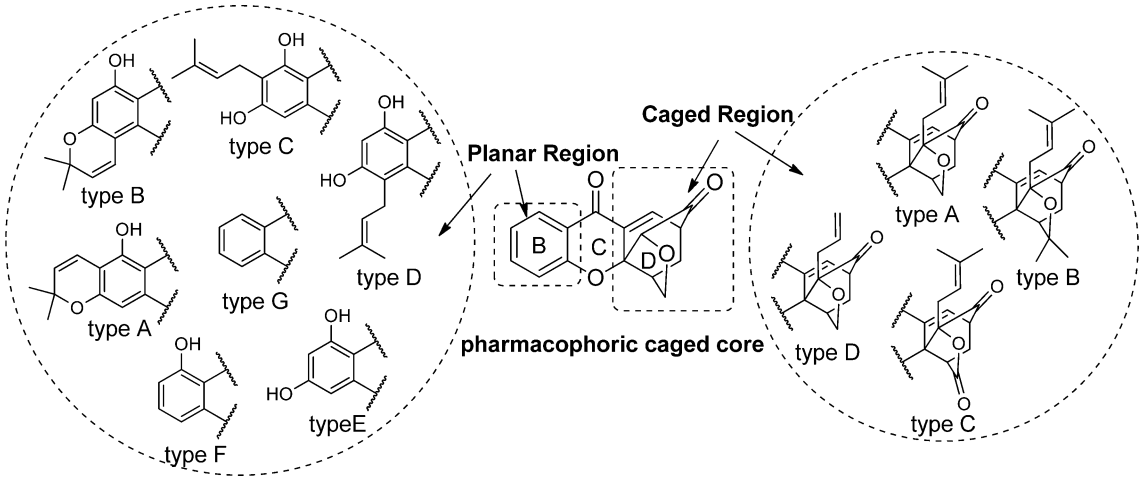

	structure		IC_{50} (μM)[a]		
compd	planar region	caged region	HepG2	A549	U251
18	type A	type A	2.99 ± 0.24	2.00 ± 0.27	12.2 ± 1.08
19	type B	type A	4.40 ± 0.14	8.43 ± 0.52	8.29 ± 0.76
20	type C	type A	3.46 ± 0.23	3.78 ± 0.25	18.7 ± 2.1
21	type D	type A	3.13 ± 0.33	2.04 ± 0.09	14.3 ± 1.9
22	type F	type A	2.65 ± 0.21	3.79 ± 0.50	23.9 ± 2.0
23	type G	type A	12.4 ± 1.1	36.1 ± 3.4	30.0 ± 2.9
29	type A	type B	2.00 ± 0.07	2.12 ± 0.18	9.62 ± 1.44
30	type B	type B	4.72 ± 0.30	3.15 ± 0.13	9.01 ± 0.66
31	type C	type B	6.27 ± 0.58	14.4 ± 1.6	22.4 ± 2.5
32	type D	type B	4.07 ± 0.09	3.58 ± 0.22	8.57 ± 0.94
28	type E	type B	3.39 ± 0.11	2.67 ± 0.39	7.32 ± 0.87
33	type F	type B	0.81 ± 0.04	0.70 ± 0.09	9.05 ± 1.17
34	type G	type B	6.77 ± 0.46	1.93 ± 0.36	18.7 ± 2.2
104	type D	type C	>100	37.9 ± 4.6	>100
36	type F	type D	9.14 ± 1.33	18.7 ± 3.8	51.7 ± 4.3

[a] **1** is the internal control for in vitro assays: HepG2, 0.89 ± 0.08 μM; A549, 1.10 ± 0.12 μM; and U251, 2.56 ± 0.25 μM.

130 (Table 3-6) with different planar regions was designed and synthesized to further explore in detail the caged region with various substituents and to improve the druglike properties by introducing hydrophilic groups.

*a. Garcinia Natural-Product-Like D-Ring-Modified Caged Xanthones **46**–**59** with a Pyran Ring in the Planar Region.* To gain insight on how modification of the D caged ring can affect cytotoxicity when the planar region features type A and B structures, HepG2, A549, and U251 cells were treated with the designed compounds **46**–**59**. As shown in Table 3, all the compounds were found to be less sensitive to U251 cells than to HepG2 and A549 cells. Compared with compound **18**, all of the compounds with pyran ring at C2 (compounds **46**–**52**) were less cytotoxic against the three cancer cell lines with the exception of **52** (IC_{50} = 0.91 μM), which was 3.2 times more active than **18** against HepG2 cells. Compared with compound **19**, all of the compounds with a pyran ring at C4 (compounds **53**–**59**) were less cytotoxic against HepG2 and U251 cells. The introduction of morpholino, $(n\text{-Pr})_2N$, $(i\text{-Pr})_2N$, or $(n\text{-Bu})_2N$ groups (compounds **55**, **57**–**59**) led to a 1.2–3.0-fold increase in activity as compared to **19**, with IC_{50} values ranging from 2.16 to 7.25 μM against A549 cells, but they were all less active than **1**. The presence of a pyrrolidinyl or Et_2N group in the caged region resulted in complete loss of cytotoxicity against the three cancer cell lines. Generally, in the case of compounds with a pyran ring in the planar region, the introduction of additional amino groups to the D caged ring contributed little to improvement of the cytotoxicity.

*b. Garcinia Natural-Product-Like D-Ring-Modified Caged Xanthones **60**–**81** with a C2 Prenyl Group in the Planar Region.* To gain insight on how modification of the D caged ring can affect cytotoxicity in compounds with a planar region featuring a type C structure, HepG2, A549, and U251 cells were incubated with the designed compounds **60**–**81**. As shown in Table 4, these compounds were generally more potent than the compounds mentioned above with pyran ring in the planar region. They were also found to be less sensitive to U251 cells than to HepG2 and A549 cells. In HepG2 cells, compared with compound **20**, seven compounds (**60**, **63**–**65**, **69**, **72**, **81**) had increased potency with IC_{50} values ranging from 1.74 to 3.16 μM. These compounds all had an alkylamino group substitution such as pyrrolidinyl, piperazinyl, methylpiperazinyl, 4-oxopiperidinyl, $(n\text{-Pr})_2N$, $(HOCH_2CH_2)_2N$, or phenylpiperazinyl groups. Another set of compounds (**61**–**62**, **67**–**68**, **71**) with alkylamino group substitution had activities comparable to that of **20**. Introduction of an *i*-PrO- group, as in compound **73**, gave a similar cytotoxicity when compared to **20**. An increase of the volume of the substituted alkyloxy group as in compounds **75** and **76** led to a decrease in activity compared to **73**. Introduction of ester groups caused a 3–6-fold

dx.doi.org/10.1021/jm301593r | J. Med. Chem. 2013, 56, 276–292

Table 3. SAR Focused on the Caged Region Containing the Pyran Ring

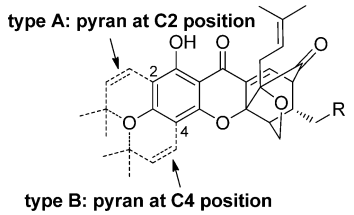

compd	planar region	R	IC_{50} (μM)[a]		
			HepG2	A549	U251
46	type A	pyrrolidin-1-yl	71.3 ± 5.7	70.3 ± 6.5	70.3 ± 5.4
47	type A	piperidin-1-yl	71.3 ± 4.3	70.3 ± 6.2	59.1 ± 3.9
48	type A	morpholino	8.82 ± 1.08	1.79 ± 0.18	12.2 ± 1.7
49	type A	Et_2N	50.4 ± 3.6	>100	>100
50	type A	$(n\text{-Pr})_2N$	5.05 ± 0.97	36.7 ± 3.2	16.8 ± 1.5
51	type A	$(i\text{-Pr})_2N$	7.93 ± 0.27	17.8 ± 1.1	>100
52	type A	$(n\text{-Bu})_2N$	0.93 ± 0.08	29.6 ± 2.6	>100
53	type B	pyrrolidin-1-yl	>100	>100	>100
54	type B	piperidin-1-yl	91.5 ± 4.0	24.9 ± 2.1	>100
55	type B	morpholino	9.35 ± 0.82	2.82 ± 1.7	13.2 ± 1.6
56	type B	Et_2N	>100	>100	>100
57	type B	$(n\text{-Pr})_2N$	5.93 ± 0.33	2.16 ± 0.06	40.4 ± 4.2
58	type B	$(i\text{-Pr})_2N$	14.5 ± 1.2	7.25 ± 0.45	23.8 ± 2.3
59	type B	$(n\text{-Bu})_2N$	9.44 ± 0.54	6.01 ± 1.07	10.7 ± 1.4

[a]Compounds **1**, **18**, and **19** are internal controls. For **1**: HepG2, 0.89 ± 0.08 μM; A549, 1.1 ± 0.12 μM; U251, 2.56 ± 0.25 μM. For **18**: HepG2, 2.99 ± 0.24 μM; A549, 2.00 ± 0.27 μM; U251, 12.2 ± 1.08 μM. For **19**: HepG2, 4.40 ± 0.14 μM; A549, 8.43 ± 0.52 μM; U251, 8.29 ± 0.76 μM.

Table 4. SAR Focused on the Caged Region Containing the Prenyl Side Chain at C2

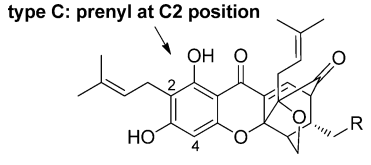

compd	R	IC_{50} (μM)[a]		
		HepG2	A549	U251
60	pyrrolidin-1-yl	2.42 ± 0.09	3.10 ± 0.24	58.6 ± 4.4
61	piperidin-1-yl	3.97 ± 0.15	6.95 ± 0.98	25.1 ± 3.0
62	morpholino	6.27 ± 1.02	35.9 ± 2.8	36.4 ± 4.2
63	piperazin-1-yl	3.16 ± 0.97	8.58 ± 1.03	31.0 ± 4.7
64	4-methylpiperazin-1-yl	2.28 ± 0.34	10.4 ± 1.3	64.6 ± 2.9
65	4-oxopiperidin-1-yl	1.74 ± 0.05	17.3 ± 2.0	58.0 ± 4.3
66	3,4-dioxopyrrolidin-1-yl	52.0 ± 7.3	16.6 ± 1.4	83.1 ± 7.8
67	Me_2N	4.28 ± 0.22	17.3 ± 0.9	45.4 ± 5.1
68	Et_2N	3.86 ± 0.30	18.0 ± 2.1	26.0 ± 2.4
69	$(n\text{-Pr})_2N$	3.13 ± 0.25	11.7 ± 1.5	79.2 ± 6.1
70	$(i\text{-Pr})_2N$	11.0 ± 1.3	3.25 ± 0.22	37.1 ± 2.6
71	$(n\text{-Bu})_2N$	4.77 ± 0.31	19.4 ± 2.1	>100
72	$(HOCH_2CH_2)_2N$	2.94 ± 0.18	9.85 ± 0.68	62.7 ± 5.2
73	*i*-PrO	3.93 ± 0.40	12.9 ± 0.7	11.7 ± 1.5
74	$HOCH_2CH_2O$	15.7 ± 1.9	58.2 ± 5.6	43.2 ± 2.9
75	$PhCH_2O$	4.84 ± 0.72	5.18 ± 0.55	17.2 ± 1.4
76	$PhCH_2CH_2O$	20.8 ± 1.4	9.12 ± 0.51	10.4 ± 1.1
77	AcO	20.5 ± 2.2	50.7 ± 4.5	21.6 ± 1.6
78	PhCOO	10.8 ± 0.8	7.34 ± 0.63	6.56 ± 0.47
79	$PhCH_2COO$	12.6 ± 1.1	6.02 ± 0.71	13.8 ± 1.5
80	PhCH═CHCOO	20.1 ± 1.7	27.1 ± 2.3	27.4 ± 3.1
81	4-phenylpiperazin-1-yl	3.10 ± 0.06	3.23 ± 0.17	63.4 ± 5.9

[a]Compounds **1** and **20** are internal controls. For **1**: HepG2, 0.89 ± 0.08 μM; A549, 1.10 ± 0.12 μM; U251, 2.56 ± 0.25 μM. For **20**: HepG2, 3.46 ± 0.23 μM; A549, 3.78 ± 0.25 μM; U251, 18.7 ± 2.1 μM.

dx.doi.org/10.1021/jm301593r | J. Med. Chem. 2013, 56, 276−292

Table 5. SAR Focused on the Caged Region Containing a Prenyl Side Chain at C4

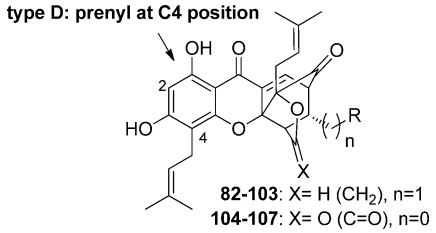

compd	R	IC_{50} (μM)[a]		
		HepG2	A549	U251
82	pyrrolidin-1-yl	4.71 ± 0.17	8.41 ± 0.44	17.1 ± 0.9
83	piperidin-1-yl	8.37 ± 0.39	5.14 ± 0.32	27.8 ± 1.7
84	morpholino	4.42 ± 0.22	8.06 ± 0.68	33.1 ± 2.2
85	piperazin-1-yl	2.56 ± 0.15	17.9 ± 1.5	35.1 ± 2.1
86	4-methylpiperazin-1-yl	4.65 ± 0.40	10.5 ± 0.7	71.6 ± 4.6
87	4-oxopiperidin-1-yl	10.6 ± 0.7	6.30 ± 0.55	>100
88	3,4-dioxopyrrolidin-1-yl	2.33 ± 0.12	5.48 ± 0.34	>100
89	Me_2N	3.92 ± 0.33	6.30 ± 0.47	21.2 ± 3.1
90	Et_2N	2.00 ± 0.02	7.61 ± 0.08	25.1 ± 2.8
91	$(n\text{-Pr})_2N$	4.60 ± 0.50	4.36 ± 0.11	24.3 ± 2.2
92	$(i\text{-Pr})_2N$	2.90 ± 0.14	3.45 ± 0.15	>100
93	$(n\text{-Bu})_2N$	3.96 ± 0.44	5.66 ± 0.63	17.3 ± 2.1
94	$(HOCH_2CH_2)_2N$	3.08 ± 0.29	3.83 ± 0.31	33.9 ± 2.7
95	*i*-PrO	2.20 ± 0.09	7.92 ± 0.66	7.48 ± 0.83
96	$HOCH_2CH_2O$	16.7 ± 2.5	28.5 ± 1.9	43.2 ± 3.2
97	$PhCH_2O$	2.22 ± 0.13	2.50 ± 0.09	22.1 ± 1.6
98	$PhCH_2CH_2O$	13.4 ± 2.0	4.78 ± 0.67	17.5 ± 2.3
99	AcO	2.95 ± 0.13	10.7 ± 1.2	13.2 ± 1.8
100	PhCOO	2.13 ± 0.20	1.13 ± 0.10	16.7 ± 2.4.
101	$PhCH_2COO$	3.28 ± 0.25	2.13 ± 0.09	9.46 ± 1.07
102	PhCH═CHCOO	21.2 ± 2.4	30.2 ± 2.7	41.4 ± 3.5
103	4-phenylpiperazin-1-yl	1.96 ± 0.12	3.07 ± 0.21	37.2 ± 3.5
104	H	>100	37.9 ± 3.6	>100
105	Me	>100	34.9 ± 3.1	>100
106	CH_3OOC	>100	>100	>100
107	Ph	>100	>100	>100

[a]Compounds **1** and **21** are internal controls. For **1**: HepG2, 0.89 ± 0.08 μM; A549, 1.10 ± 0.12 μM; U251, 2.56 ± 0.25 μM. For **21**: HepG2, 3.13 ± 0.33 μM; A549, 2.04 ± 0.09 μM; U251, 14.3 ± 1.9 μM.

decrease in activity. In A549 cells, most of the compounds were found to be less active when compared to compound **20**, and only three compounds (**60**, **70**, **81**) were more cytotoxic. In U251 cells, five compounds (**73**, **75**−**76**, **78**−**79**) with hydrophobic group substitution in the caged region showed greater activity than compound **20**. These results suggest that in the case of compounds with a C2 prenyl group in the planar region, the introduction of hydrophilic alkylamino groups to the caged D-ring generally increased cytotoxicity against HepG2 cells while introduction of hydrophobic and bulky groups led to a decrease in activity. The presence of substituents in the caged region was generally unfavorable to antitumor activity against A549 and U251 cells.

*c. Garcinia Natural-Product-Like D-Ring-Modified Caged Xanthones **82**−**107** with a C4 Prenyl Group in the Planar Region.* To gain insight on how modification of the D caged ring can affect cytotoxicity when the planar region features a type D structure, HepG2, A549, and U251 cells were incubated with the designed compounds **82**−**107**. As shown in Table 5, compared with compound **21**, 10 compounds (**85**, **88**, **90**, **92**, **94**−**95**, **97**, **99**−**100**, **103**) had increased potency against HepG2 cells with IC_{50} values ranging from 1.96 to 3.08 μM, and most of these compounds showed decreased cytotoxicity against A549 and U251 cells. The substitution of the *gem*-dimethyl group linked to the caged scaffold by an electron-withdrawing carbonyl group interfered significantly with the cytotoxicity, in all three cancer cell lines, as observed for compounds **104**−**107**. Among compounds **82**−**103**, the substitution of the alkylamino group led to increased or maintained cytotoxicity against HepG2 cells. When introducing some alkyloxy or ester groups, compounds **95**, **97**, **99**, **100** were obtained and had improved activity against HepG2 cells. The cytotoxicity was improved when the substituent groups contained an aromatic ring, as observed for compounds **97** and **100**−**101** with IC_{50} values ranging from 1.13 to 3.28 μM against HepG2 and A549 cells. However, replacement of substituents by the long-chain alkyloxy or ester groups as in compounds **98** and **102** caused a significant decrease in activity against HepG2 and A549 cells. Compound **112** with a phenylpiperazinyl group was synthesized to determine if the length of the substituents affected the cytotoxicity and whether the alkylamino group may improve the physicochemical property of the molecules. Compound **112** showed the most potent cytotoxicity against HepG2 cells with an IC_{50} value of

dx.doi.org/10.1021/jm301593r | J. Med. Chem. 2013, 56, 276−292

Table 6. SAR Focused on the Caged Region Containing a Simplified B-Ring

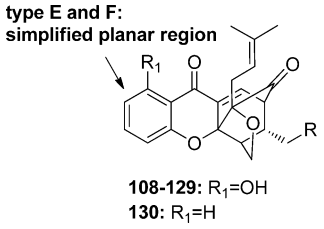

108-129: R_1=OH
130: R_1=H

compd	R	IC_{50} (μM)[a] HepG2	A549	U251
108	pyrrolidin-1-yl	8.82 ± 0.77	12.5 ± 1.0	>100
109	piperidin-1-yl	12.1 ± 1.1	10.2 ± 0.8	>100
110	morpholino	7.72 ± 0.45	8.51 ± 0.34	>100
111	piperazin-1-yl	7.50 ± 0.43	4.24 ± 0.27	>100
112	4-methylpiperazin-1-yl	3.25 ± 0.22	3.60 ± 0.19	71.0 ± 5.7
113	4-oxopiperidin-1-yl	2.59 ± 0.31	9.14 ± 0.48	>100
114	3,4-dioxopyrrolidin-1-yl	10.2 ± 0.6	38.0 ± 2.58	>100
115	Me_2N	8.59 ± 0.71	38.2 ± 2.41	>100
116	Et_2N	7.89 ± 0.73	20.5 ± 2.17	>100
117	$(n\text{-Pr})_2N$	3.69 ± 0.26	7.82 ± 0.33	>100
118	$(i\text{-Pr})_2N$	33.1 ± 2.08	23.5 ± 2.26	>100
119	$(n\text{-Bu})_2N$	7.83 ± 0.63	1.25 ± 0.06	94.9 ± 3.3
120	$(HOCH_2CH_2)_2N$	6.53 ± 0.48	9.68 ± 0.70	>100
121	MeO	5.70 ± 0.35	14.8 ± 1.4	>100
122	*i*-PrO	5.21 ± 0.32	37.3 ± 3.5	>100
123	$PhCH_2O$	7.21 ± 0.48	5.83 ± 1.01	93.1 ± 5.1
124	$PhCH_2CH_2O$	>100	4.46 ± 0.29	>100
125	AcO	23.9 ± 1.7	36.3 ± 4.0	>100
126	PhCOO	11.8 ± 0.8	10.9 ± 1.1	>100
127	$PhCH_2COO$	6.65 ± 0.12	7.58 ± 0.33	>100
128	PhCH=CHCOO	24.8 ± 2.2	14.9 ± 1.3	>100
129	4-phenylpiperazin-1-yl	7.34 ± 0.34	2.15 ± 0.17	>100
130	4-methylpiperazin-1-yl	41.6 ± 4.3	54.0 ± 3.6	>100

[a]Compounds **1** and **22** are internal controls. For **1**: HepG2, 0.89 ± 0.08 μM; A549, 1.10 ± 0.12 μM; U251, 2.56 ± 0.25 μM. For **22**: HepG2, 2.65 ± 0.21 μM; A549, 3.79 ± 0.50 μM; U251, 23.9 ± 2.0 μM.

1.96 μM and also inhibited A549 cells with an IC_{50} value of 3.07 μM. These results suggest that in the case of compounds with a C4 prenyl group in the planar region, the introduction of hydrophilic alkylamino groups to the caged D-ring can also increase cytotoxicity against HepG2 cells. The presence of aromatic substitutents in the caged region seemed to be favorable for antitumor activity against HepG2 and A549 cells, while the length and volume of the substituted moiety in the caged region affected the cytotoxicity significantly. Furthermore, replacement of the *gem*-dimethyl group linked to the caged scaffold by a carbonyl group caused loss in activity against all the three cancer cells.

*d. Garcinia Natural-Product-Like D-Ring-Modified Caged Xanthones **108**–**130** Containing a Simplified Planar Region.* To gain insight on how modification of the D caged ring can affect the cytotoxicity when the planar region features a type E structure, HepG2, A549, and U251 cells were incubated with the designed compounds **108**–**129**. As shown in Table 6, a better selectivity for HepG2 and A549 cells was achieved, since all the compounds were nearly inactive against U251 cells even at a concentration of 100 μM. This series of compounds was generally less active than the corresponding analogues that have prenyl substitution in the planar region. Although compared with compound **22**, most of the compounds showed less potency against HepG2 and A549 cells, these simplified analogues generally were inhibitory at micromolar levels and had improved druglike properties (see Table 7). Notably, 15 of them had IC_{50} values against HepG cells below 10 μM, while the number was decreased to 10 in the case of A549 cells. Introduction of hydrophilic alkylamino groups, such as methylpiperazinyl, 4-oxopiperidinyl, and $(n\text{-Pr})_2N$ groups, as in compounds **112**, **113**, and **117**, respectively, led to a similar cytotoxic profile when compared to compound **22**. Compound **112** showed comparable cytotoxicity against HepG2 and A549 cells with an IC_{50} value of 3.25 and 3.60 μM, respectively. Meanwhile, compounds **121**–**123**, with alkyloxy substituents, also exhibited cytotoxicity, whereas further introducing long-chain alkyloxy group as in compound **124** resulted in major loss of activity against HepG2 cells. A similar decrease in cytotoxicity was also observed in compound **128** as compared to **126** and **127**. The bulky substituent seemed to increase the activity against A549 cells, since compound **119** with a $(n\text{-Bu})_2N$ group showed the most potent activity against A549 cells among all these series of compounds. Introduction of long-chain aromatic moieties as in compounds **124**, **127**–**129** did not interfere significantly with the cytotoxicity to A549 cells. Removal of the C1 hydroxyl substituent in compound **112** produced the significantly less active compound **130.** This was consistent with the finding that the presence of a hydroxyl group at C1 improved the cytotoxicity. These results suggest that in the case of compounds with a simplified planar region, the introduction of alkylamino, alkyloxyl, or ester groups to caged D-ring generally led to sustained antitumor activity and facilitated improvement of the physicochemical properties such as water solubility and cell member permeability while having little effect on cytotoxicity, since the structures of these natural-product-like caged xanthones were greatly simplified compared to the natural product GA.

Structure–Property Relationship Studies. In parallel with the antitumor activity testing, the physicochemical properties of 40 representative diverse caged compounds were determined in an effort to identify potential druglike compounds prior to the time-consuming and costly development and optimization of analogues that may ultimately fail in in vivo efficacy experiments. Compound **1** was used as a reference compound for comparison of polar surface area, log $D_{7.4}$, intrinsic aqueous solubility, and permeability (Table 7). Digoxin and propranolol were used as internal standards for permeability. The polar surface area (PSA) was calculated by Discovery Studio 3.0 using the ADMET protocol. The partition coefficient (log *D*) at pH 7.4 and aqueous solubility were determined according to the method of Avdeef and Tsinman[52] on a Gemini Profiler instrument (pION) by the "gold-standard" Avdeef–Bucher potentiometric titration method.[53] Permeability coefficients were determined using a standard parallel artificial membrane permeability assay (PAMPA) on a PAMPA Explorer instrument (pION).

As shown in Table 7, all the synthetic caged compounds displayed aqueous solubility that was improved over that of **1**. Among all the tested compounds, compound **120** was the most soluble with an intrinsic solubility of 10.37 mM, almost 1000 times more soluble than **1**. Generally, the introduction of

dx.doi.org/10.1021/jm301593r | J. Med. Chem. 2013, 56, 276–292

Table 7. SPR Focused on both the Planar and Caged Regions

	structure						
compd	planar region	caged region	R	PSA_2D (Å^2)	log *D*, pH 7.4	intrinsic solubility, (mM)	P_e, pH 7.4 (10^{-6} cm/s)[a]
18	type A	type A	—	82.2	4.0	0.32	16.8
48	type A	type E	morpholino	94.5	3.8	0.84	26.4
52	type A	type E	$(n\text{-Bu})_2N$	85.6	6.2	0.028	8.1
19	type B	type A	—	82.2	4.3	0.17	13.6
55	type B	type E	morpholino	94.5	4.0	0.43	36.3
59	type B	type E	$(n\text{-Bu})_2N$	85.6	6.0	0.021	8.2
20	type C	type A	—	94.1	3.6	0.57	21.9
60	type C	type E	pyrrolidin-1-yl	97.4	3.9	0.98	26.2
62	type C	type E	morpholino	106.4	3.1	1.27	28.4
67	type C	type E	Me_2N	97.4	2.4	2.19	12.2
71	type C	type E	$(n\text{-Bu})_2N$	97.4	4.7	0.71	22.7
72	type C	type E	$(HOCH_2CH_2)_2N$	139.1	2.6	4.52	9.1
81	type C	type E	4-phenylpiperazin-1-yl	100.8	4.5	0.38	13.2
21	type D	type A	—	94.1	3.5	0.50	12.1
32	type D	type B	—	94.1	3.9	0.34	10.3
82	type D	type E	pyrrolidin-1-yl	97.4	3.7	0.85	15.6
83	type D	type E	morpholino	106.4	3.2	1.25	27.3
89	type D	type E	Me_2N	97.4	2.6	2.45	41.9
93	type D	type E	$(n\text{-Bu})_2N$	94.4	5.1	0.092	11.8
94	type D	type E	$(HOCH_2CH_2)_2N$	139.1	2.0	4.32	19.0
103	type D	type E	4-phenylpiperazin-1-yl	100.8	4.7	0.34	20.6
95	type D	type E	*i*-PrO	103.0	3.6	0.32	23.5
97	type D	type E	$PhCH_2O$	103.0	4.9	0.16	11.0
99	type D	type E	AcO	120.3	2.8	0.83	34.2
101	type D	type E	$PhCH_2COO$	120.3	5.1	0.21	9.8
28	type E	type B	—	94.1	2.3	1.41	27.5
33	type F	type B	—	73.3	2.9	0.84	77.6
34	type G	type B	—	52.5	—[b]	—[b]	29.3
108	type F	type E	pyrrolidin-1-yl	76.6	2.9	2.00	108.1
110	type F	type E	morpholino	85.6	2.0	3.88	153.2
111	type F	type E	piperazin-1-yl	89.4	0.44	5.79	37.2
112	type F	type E	4-methylpiperazin-1-yl	80.0	1.8	4.80	155.7
115	type F	type E	Me_2N	76.6	1.7	7.01	189.1
119	type F	type E	$(n\text{-Bu})_2N$	76.6	4.6	0.19	50.1
120	type F	type E	$(HOCH_2CH_2)_2N$	118.3	1.2	10.37	197.2
129	type F	type E	4-phenylpiperazin-1-yl	80.0	3.6	0.62	77.3
122	type F	type E	*i*-Pr	82.2	2.9	1.06	123.2
123	type F	type E	$PhCH_2O$	82.2	3.5	0.57	82.5
125	type F	type E	AcO	99.5	1.9	5.44	143.3
127	type F	type E	$PhCH_2COO$	99.5	3.6	0.64	67.3
1	—	—	—	120.3	3.6	0.015	26.5

[a]Digoxin (30.0×10^{-6} cm/s) and propranolol (541.5×10^{-6} cm/s) are internal standards in permeability determinations. [b]Undetermined

hydrophilic groups such as morpholino, pyrrolidin-1-yl, piperazin-1-yl, and 4-methylpiperazin-1-yl resulted in a significant increase in solubility. For instance, comparing the solubility of **52** and **48**, **55** and **19**, **67** and **20**, **120** and **33**, showed that all the former compounds were more soluble than the latter compounds. Introduction of hydrophobic aliphatic chains such as dibutylamino and benzyl groups with bulk volume led to poor solubility. For examples, compounds **52**, **59**, **71**, and **119** with dibutylamino substitution, compounds **97** and **123** with a benzyloxy group, and compounds **101** and **127** with a phenylacetoxy group all displayed reduced aqueous solubility compared to the corresponding analogues lacking these substituents. Furthermore, it was shown that compounds with a simplified planar region (type F) were far more soluble than compounds with a prenyl substituent (types C and D) or fused pyran ring (types A and B) in the planar region. Compounds of type A and B planar regions showed the poorest solubility, probably a result of the increased rigidity of the molecule due to the additional pyran ring. These results suggest that compounds with a smaller framework and with hydrophilic groups are likely to have better aqueous solubility.

Permeability is another important property reflecting the ability of molecules to diffuse through the cell membrane. Generally, as shown in Table 7, the P_e values of all compounds were less than that of the positive control compound, propranolol. Compound **115**, the most permeable of the caged xanthone analogues, had a P_e value of 189.1×10^{-6} cm/s. Compounds with simple B-ring, such as those with a type F planar region, possessed better permeability when compared to those with prenyl or pyran substituents in the planar region. In addition, the introduction of hydrophilic groups to the caged region of the molecules also led to an improvement in

dx.doi.org/10.1021/jm301593r | J. Med. Chem. 2013, 56, 276−292

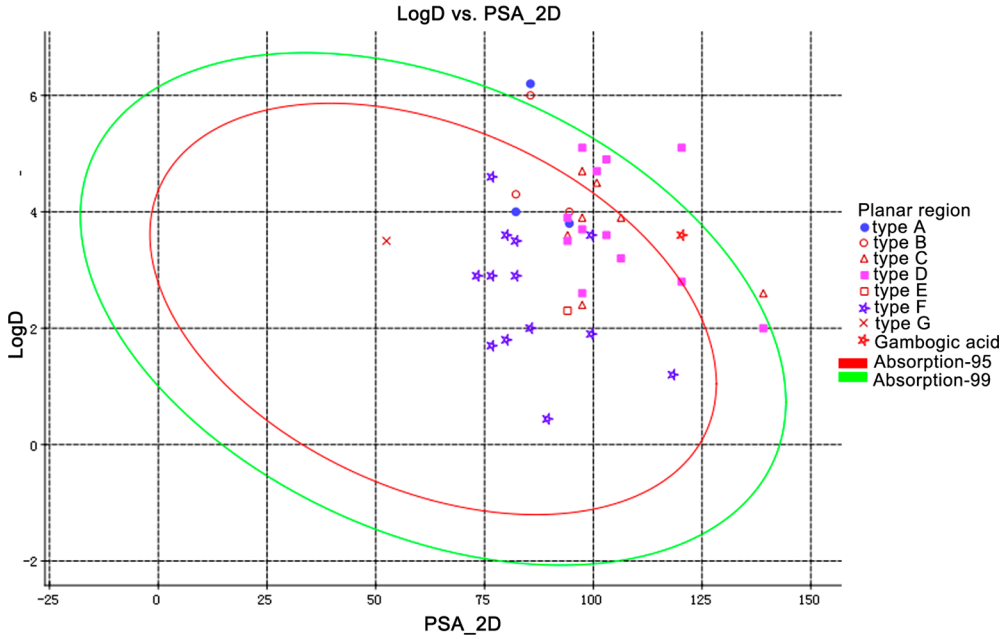

Figure 3. Plot of log *D* (pH 7.4) versus PSA_2D.

Table 8. Inhibitory Effect of 103, 112, 33, and 1 with iv Administration on the Growth of Heps Transplanted Mice

		body weight (g)			
group	dose (iv) (mg/kg)	predose	postdose	weight of tumor (g)	inhibitory rate (%)
control	0	20.75 ± 1.20	29.75 ± 3.03	1.27 ± 0.20	0.00
103	20	20.88 ± 1.69	28.50 ± 1.50	0.88 ± 0.51	30.74
103	40	21.75 ± 1.92	27.43 ± 4.53	0.65 ± 0.16^b	48.77
103	80	21.50 ± 1.32	26.50 ± 2.50	0.51 ± 0.22^b	60.20
112	5	21.10 ± 1.30	29.25 ± 1.56	0.62 ± 0.18^b	45.67
112	10	22.00 ± 1.56	27.71 ± 4.27	0.50 ± 0.26^b	56.06
112	20	21.56 ± 0.68	27.22 ± 2.53	0.48 ± 0.15^b	57.75
33	10	20.67 ± 1.41	27.33 ± 5.54	0.95 ± 0.27^a	25.21
33	20	21.44 ± 2.87	28.11 ± 4.33	0.83 ± 0.19^b	34.49
33	40	20.13 ± 1.27	26.43 ± 3.50	0.75 ± 0.39^b	40.66
1	10	22.50 ± 1.20	28.00 ± 4.56	0.35 ± 0.17^b	69.11
5-FU	25	19.50 ± 1.32	21.17 ± 4.14	0.38 ± 0.22^b	70.31

$^a P < 0.05$. $^b P < 0.01$ vs control.

permeability. Compounds such as **52**, **59**, **97**, **101**, **119**, and **123**, with bulky hydrophobic substituents, were found to have poor permeability when compared to the analogues lacking these substituents. These results suggest that the trends of permeabilities of these compounds are similar to the solubilities; compounds with smaller frameworks and hydrophilic groups are also likely to have better permeability.

Whether a drug can be well-absorbed intestinally after oral administration depends on the intrinsic properties of the molecule, and the polar surface area and distribution coefficient are the two main aspects. Egan et al. developed an intestinal absorption model using 182 compounds with descriptors that include AlogP and 2D polar surface area (PSA_2D).[54,55] In this model, the compounds that are well-absorbed will generally reside within the elliptical regions of 95% (in red) and 99% (in green) confidence levels (Figure 3). Analysis of a plot of the measured log *D* versus the calculated PSA_2D of the selected cage xanthones (Figure 3) showed that most of the compounds with type F structure in the planar region fell within the ellipse regions of 95% while GA fell outside the ellipse regions of 95%. These results are consistent with the permeability data and suggest that the compounds with good permeability such as compounds with type F planar region are likely to have favorable intestinal absorption.

In vivo Antitumor Activity with iv Administration. Both the in vitro antitumor activity and physicochemical properties have been taken into account when determining whether a compound is druglike and has potential to be active in vivo. For instance, compound **52**, which features a pyran ring in the plannar region, possessed a low micromolar activity against HepG2 cells (IC_{50} = 0.93 μM), but it had poor aqueous solubility (0.028 mM) and cell member permeability (8.1 × 10^{-6} cm/s), thus compound **52** fell out of favor for further in vivo evaluation. Compound **103**, which features a prenyl group in the plannar region, showed potent in vitro activity against HepG2 cells (IC_{50} = 1.96 μM) and had an improved aqueous solubility (0.34 mM) as compared to **1**, and as a consequence, compound **103** was selected to be advanced into in vivo efficacy experiments. Although compound **112** had moderate potency in vitro against HepG2 cells (IC_{50} = 3.25 μM), it

dx.doi.org/10.1021/jm301593r | J. Med. Chem. 2013, 56, 276−292

features a much smaller molecular size and possessed greatly improved solubility (4.8 mM) and permeability (155.7×10^{-6} cm/s) as compared to **1**. Besides, statistic data showed that the polar surface area (PSA) for 1590 orally administered non-CNS drugs that have reached at least phase II efficacy studies mainly distribute between 60 and 80 Å^2 and that compounds with large PSA (>120 Å^2) are hardly absorbed by the passive transcellular route.[56] The PSA value of compound **112** (80.0 Å^2) fitted well with the requirement of orally administered drugs. On the basis of the above consideration, compound **112** was expected to be potentially active in vivo.

In the light of the in vitro antitumor activity and physicochemical properties, we selected compounds **103** and **112** to determine their in vivo efficacy with iv administration on the growth of hepatoma solidity (Heps) in mice using **1**, 5-fluorouracil (5-FU), and a previously studied[38] caged xanthone analogue **33** for comparison. As shown in Table 8, the tumor growth inhibitory rates of **1** and 5-FU were 69.11% and 70.31%, at 10 and 25 mg/kg twice daily doses, over a period of 8 days, respectively. Compounds **103** and **112** displayed significant inhibitory effect on the growth of inoculated Heps in mice in a dose-dependent manner, with 48.77% and 56.06% inhibitory in tumor growth, at 40 and 10 mg/kg twice daily doses, respectively. Whereas the inhibitory rate was only 40.66% when administrated with compound **33** at 40 mg/kg twice daily dose. Although **103** (IC_{50} = 1.96 μM) and **112** (IC_{50} = 3.25 μM) were less active than **33** (IC_{50} = 0.81 μM) against HepG2 cells in vitro, they both were found to be more effective than **33** in vivo. Moreover, compound **112**, with the lowest in vitro activity of three caged analogues against HepG2 cells, turned out to the most potent compound in vivo on inhibition of the growth of inoculated Heps in mice. This may be attributed to the improved physicochemical properties such as aqueous solubility and cell membrane permeability of **112** compared to **103** and **33**. No vascular irritation or weight loss was observed in any of these in vivo tests.

Pharmacokinetic Data. The compounds with effective in vivo antitumor activity were evaluated for their in vivo pharmacokinetic parameters to determine which compounds are potentially orally active. The natural product GA was tested for comparison. The full in vivo PK parameters for **103**, **112**, **33**, and **1** in CD-1 mice are presented in Table 9. Compared with **1**, the simplified xanthones **33** and **103** showed relative shorter $t_{1/2}$ values, with a higher clearance and distribution volume. Compound **112** had a $t_{1/2}$ value similar to that of **1** and significantly increased distribution volume, indicating the possibility of wide distribution. With oral dosing, shorter t_{max} values were observed in compounds **33** and **103** (0.25 h) compared to **1** (0.5 h), while compound **112** had the same t_{max} value as **1**. Oral bioavailability of the simplified xanthone **33** (2.59%) was much less than that of **1** (13.4%). Introduction of hydrophilic amino moieties led to an increase in oral bioavailability as observed in compounds **103** and **112** compared to **33**. Compound **112**, which has a simplified planar region and hydrophilic methylpiperazinyl substituents in the caged region, had the best oral bioavailability, about 12% better than that of **1**.

Table 9. Pharmacokinetics of 103, 112, 33, and 1

	PK parameters[a]	103	112	33	1
iv	dose (mg/kg)	5	5	5	5
	$t_{1/2}$ (h)	1.60	4.34	1.41	5.06
	MRT (h)	1.44	1.81	0.53	2.26
	Cl (mL/h/kg)	22615	20521	3338	2461
	V_d (L/kg)	52.2	128.3	6.8	19.7
	AUC (ng h/mL)	205	242	1477	2005
po	dose (mg/kg)	20	20	20	20
	t_{max} (h)	0.25	0.50	0.25	0.50
	C_{max} (ng/mL)	14.9	79.6	1.46	191
	$t_{1/2}$ (h)	2.62	1.12	1.36	3.29
	MRT (h)	2.28	1.63	0.947	4.51
	AUC (ng h/mL)	40	151	153	1072
	F (%)	4.88	15.6	2.59	13.4

[a]Determinations with three mice per time point, average value.

In vivo Antitumor Activity with po Administration. Considering both the in vivo antitumor activity with iv administration and the pharmacokinetic data described above, we selected compound **112** to determine further its in vivo efficacy with po administration on the growth of hepatoma solidity (Heps) in mice using **1** as comparison control. As shown in Table 10, compound **112** displayed much more inhibitory potency on the growth of inoculated Heps in mice, while the tumor weight in the control group was unchanged and neither vascular irritation nor weight loss was observed in any of the groups. For compound **112**, 57.74% inhibition in tumor growth was observed at 100 mg/kg daily oral dose, over a period of four days, while the inhibitory rate of **1** was 36.36% at the same dose. Thus, compound **112** was identified as the first orally active *Garcinia* natural-product-like caged xanthone and also a promising novel antitumor agent for further clinical development.

CONCLUSIONS

Using regioselective propargylation of diverse hydroxyxanthone substrates, we have developed a novel synthetic approach to *Garcinia* xanthones with diverse caged regions. With this synthetic strategy, we have synthesized 99 *Garcinia* structurally diverse natural-product-like xanthones containing the pharmacophoric caged core. These synthetic compounds have been used to further explore the properties of the planar B-ring and the caged D-ring of *Garcinia* analogues. All the synthesized compounds have been evaluated for their in vitro antitumor activity against HepG2, A549, and U251 cells, and detailed SAR around the pharmacophoric caged core have been determined. The intrinsic aqueous solubility, polar surface area (PSA), log $D_{7.4}$, and permeability at pH 7.4, and the detailed structure–property relationships (SPR) of a select set of 40 *Garcinia* caged xanthones have also been determined. Various hydrophilic groups have been introduced to the caged region in an effort to improve the druglike properties of the compounds. The important SAR and SPR information of these compounds is comprehensively presented in Figure 4. In the light of the in vivo antitumor activity and the measured druglike properties, two compounds, **103** and **112**, were selected for testing in in vivo efficacy experiments with iv administration. The results showed that **103** and **112** displayed a significant and dose-dependent inhibitory effect on the growth of inoculated Heps in mice, while neither vascular irritation nor weight loss was observed in any of the dose groups. In vivo pharmacokinetic parameters such as t_{max}, $t_{1/2}$, AUC, and F were determined.

Compound **112** had the best bioavailability and was chosen for determination of its antitumor potency with po administration. The results showed that **112** has more potent in vivo orally antitumor activity than GA. This novel *Garcinia*

Table 10. Inhibitory Effect of 112 and 1 with po Administration on the Growth of Heps Transplanted Mice

		body weight (g)			
group	dose (po) (mg/kg)	predose	postdose	weight of tumor (g)	inhibitory rate (%)
control	0	20.75 ± 1.20	29.75 ± 3.03	1.27 ± 0.20	0.00
112	100	22.00 ± 1.18	27.22 ± 2.53	0.48 ± 0.15[b]	57.74
1	100	21.60 ± 0.49	25.13 ± 2.98	0.73 ± 0.24[a]	36.36

[a] $P < 0.05$. [b] $P < 0.01$ vs control.

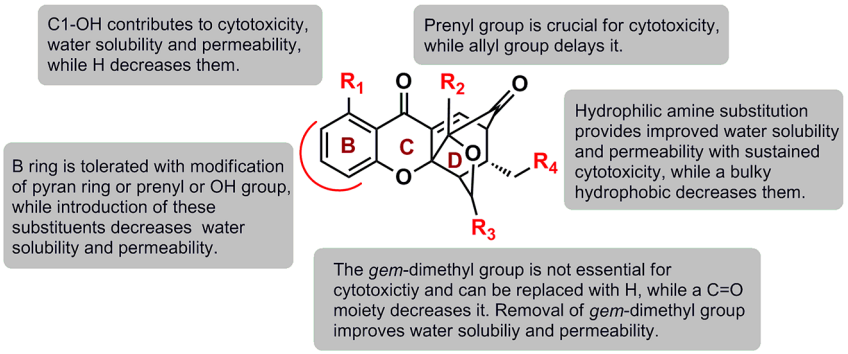

Figure 4. Graphical depiction of the general SAR for cell cytotoxicity based on the IC_{50} results on HepG2 cells and SPR for water solubility and cell membrane permeability.

natural-product-like caged xanthone is therefore an orally active antitumor agent that is promising for further clinical development.

EXPERIMENTAL SECTION

All reagents were purchased from commercial sources and, unless otherwise noted, were used without further purification. Organic solutions were concentrated in a rotary evaporator (Büchi Rotavapor) below 45 °C under reduced pressure. Reactions were monitored by thin-layer chromatography (TLC) on 0.25 mm silica gel plates (GF254) and visualized under UV light. Silica gel (60 Å, 300−400 mesh) was used for flash column chromatography. Melting points were determined with a Melt-Temp II apparatus and were reported without correction. IR spectra were recorded on a Nicolet iS10 Avatar FT-IR spectrometer using KBr film. The ^1H NMR and ^{13}C NMR spectra were measured on a Bruker AV-300 or Bruker AV-500 instrument using deuterated solvents with tetramethylsilane (TMS) as internal standard. Multiplicities were defined as s (singlet), d (doublet), t (triplet), or m (multiplet). EI-mass spectra were recorded with a Shimadzu GCMS-2010 mass spectrometer. High-resolution mass spectra (HRMS) were recorded on a Water Q-Tof micro mass spectrometer. The purity (≥95%) of the compounds was verified by the HPLC study performed on an Amethyst C18−P (4.6 × 150 mm, 5 μm, Merck) column using a mixture of solvent methanol/water or acetonitrile/water at the flow rate of 2 mL/min and peak detection at 240 nm under UV.

Cancer cell lines were obtained from Cell Bank of Shanghai, Institute of Biochemistry and Cell Biology, Chinese Academy of Sciences. Cells were cultured in 90% RPMI 1640 medium (GIBCO, Invitrogen Corp.) supplemented with 10% fetal bovine serum (Sijiqing, Zhejiang, China), 100 U/mL benzyl penicillin, and 100 μg/mL streptomycin in a humidified environment with 5% CO_2 at 37 °C. Gambogic acid was isolated from Gamboge resin according to the previously reported protocols.[6] Samples containing >95% Gambogic acid were used in the experiments. All the tested compounds were dissolved in DMSO at a concentration of 0.01 mol/L and stored at −4 °C.

Chemistry. For experimental procedures and spectral characterization data see the Supporting Information.

MTT Assay. Cell viabilities were measured by a colorimetric assay using 3-(4,5-dimethylthiazol-2-yl)-2,5-diphenyltetrazolium bromide (MTT, Roche) as described previously.[38] Experiments were carried out in triplicate in a parallel manner for each concentration of target compounds used, and the results are presented as mean ± SE. Control cells were given only culture media. After incubation for 24 h, the absorbance (A) was measured at 570 nm. Survival ratio (%) was calculated using the following equation: survival ratio (%) = ($A_{treatment}/A_{control}$) × 100%. IC_{50} was taken as the concentration that caused 50% inhibition of cell viabilities and was calculated by the SigmaPlot software (Systat Software Inc.).

PAMPA Assay. Permeability (P_e) was determined by a standard parallel artificial membrane permeability assay (PAMPA by pION). PAMPA was conducted on a PAMPA Explorer instrument (pION Inc., Woburn, MA) with PAMPA Explorer command software (Version 3.6.0.6) as follows: test compound stock was diluted with system solution buffer, pH 7.4 (pION Inc., Woburn, MA) to make diluted test compound at 2 mM concentration. Then 150 μL of diluted test compound was transferred to a UV plate (pION Inc.,Woburn, MA), and the UV spectrum was read as the reference plate. The membrane on a preloaded PAMPA sandwich (pION Inc., Woburn, MA) was painted with 4 μL of GIT lipid (pION Inc., Woburn, MA). The acceptor chamber was then filled with 200 μL of acceptor solution buffer (pION Inc., Woburn, MA), and the donor chamber was filled with 150 μL of diluted test compound. The PAMPA sandwich was assembled, placed on the Gut-Box controlled environment chamber, and stirred for 30 min. The aqueous boundary layer was set to 40 μm for stirring. The UV spectrum (200−500 nm) of the donor and the acceptor were read. The permeability coefficient was calculated using PAMPA Explorer command software (Version 3.6.0.6) based on the AUC of the reference plate, the donor plate, and the acceptor plate. All compounds were tested in triplicate, and the data are presented as an average value. Standards for this assay include digoxin (P_e = 30.0 × 10^{-6} cm/s at pH = 7.4) and propranolol (P_e = 541.5 × 10^{-6} at pH = 7.4).

In Vivo Pharmacokinetic Assay. Fifty-four healthy male CD-1 mice (weight ranging from 18 to 30 g, 27 mice for po, and 27 mice for iv) were administered with **103**, **112**, **33**, or **1**. For the po study, a single dose of 20 mg/kg body weight of **103**, **112**, **33**, and **1** was administered orally to mice. The dosing volume was 10 mL/kg. Animals were fasted approximately 16 h prior to dosing until 4 h postdosing but water was available to all animals at all times. For iv study, a single dose of 5 mg/kg body weight of **103**, **112**, **33**, and **1** was administered iv to mice. The dosing volume was 10 mL/kg. Food and water were available to animals at all times during the experiment.

dx.doi.org/10.1021/jm301593r | J. Med. Chem. 2013, 56, 276−292

Three mice were bled by cardiac puncture at each time point (0, 0.25, 0.5, 1, 1.5, 2, 4, 6, and 24 h for the po group and 0, 0.083, 0.25, 0.5, 1, 2, 4, 6, and 24 h for the iv group). Blood was collected into K_3EDTA tubes and centrifuged immediately at 4 °C at 3000 rpm for 10 min. Plasma samples were transferred and stored at −20 °C prior to analysis. The plasma samples were determined by LC−MS/MS assays.

In Vivo Tumor Growth Inhibition Assay. Kunming mice with body weight of 18−22 g were transplanted with hepatoma solidity (Heps) according to protocols of transplant tumor research; 24 h after tumor transplantation, animals were weighed and randomly divided into five groups. All test drugs were given through injections 24 h after tumor transplantation. The treated groups were iv injected or po administration of different doses of test compounds, respectively. The negative control group received 0.9% normal saline. Treatments were done at a frequency of one iv dose per 2 days or one po dose per day for a total of four treatments. All animals were sacrificed 24 h after the fourth treatment. All data are presented as the mean ± SD, and the statistical significance was evaluated by the *t*-test.

■ ASSOCIATED CONTENT

Supporting Information

Experimental procedures for synthesis and spectral data for characterization. This material is available free of charge via the Internet at http://pubs.acs.org.

■ AUTHOR INFORMATION

Corresponding Author

*Q.Y.: fax and phone, +86-25-83271351; e-mail, youqidong@gmail.com. Q.G.: fax and phone, +86-25-83271440; e-mail: anticancer_drug@yahoo.com.cn. H.S.: fax and phone, +86-25-83271216; e-mail, sunhaopeng@163.com.

Notes

The authors declare no competing financial interest.

■ ACKNOWLEDGMENTS

We are thankful for the financial support of the National Natural Science Foundation of China (No. 90713038, No. 21072231), National Major Science and Technology Project of China (Innovation and Development of New Drugs, No. 2009ZX09501-003, No. 2010ZX09401-401), and "863" Program of China (No. 2012AA020301).

■ ABBREVIATIONS USED

NP, natural product; GA, gambogic acid; Bcl-2, B-cell lymphoma 2; IκBα, nuclear factor of kappa light polypeptide gene enhancer in B-cells inhibitor alpha; SAR, structure−activity relationship; SPR, structure−property relationship; PSA_2D, 2D polar surface area; THF, tetrahydrofuran; DMF, dimethylformamide; DCM, dichloromethane; DMSO, dimethyl sulfoxide; EDC·HCl, 1-ethyl-3-(3-dimethylaminopropyl)-carbodiimide hydrochloride; DMAP, 4-dimethylaminopryidine; MTT, 3-(4,5-dimethylthiazol-2-yl)-2,5-diphenyltetrazolium bromide; IC_{50}, half-maximal inhibitory concentration; Me, methyl; Et, ethyl; Pr, propyl; Bu, butyl; Ph, phenyl; Ac, acetyl; Me_2CO, acetone; ADMET, aborption distribution metabolism excretion toxicity; PAMPA, parallel artificial membrane permeation assay; P_e, permeability coefficient; CNS, central nervous system; iv, intravenous injection; 5-FU, 5-fluorouracil; po, per os (oral) ; $t_{1/2}$, half-life; MRT, mean residence time; Cl, clearance; V_d, volume of distribution; AUC, area under curve; C_{max}, peak concentration; *F*, bioavailability; Heps, hepatoma solidity.

■ REFERENCES

(1) Newman, D. J.; Cragg, G. M. Natural products as sources of new drugs over the 30 years from 1981 to 2010. *J. Nat. Prod.* **2012**, *75*, 311−335.
(2) Butler, M. S. Natural products to drugs: Natural product-derived compounds in clinical trials. *Nat. Prod. Rep.* **2008**, *25*, 475−516.
(3) Mishra, B. B.; Tiwari, V. K. Natural products: An evolving role in future drug discovery. *Eur. J. Med. Chem.* **2011**, *46*, 4769−4807.
(4) Auterhoff, H.; Frauendorf, H.; Liesenklas, W.; Schwandt, C. The chief constituents of gamboges resin. 1. Chemistry of gamboge. *Arch. Pharm.* **1962**, *295*, 833−846.
(5) Han, Q. B.; Xu, H. X. Caged *Garcinia* xanthones: Development since 1937. *Curr. Med. Chem.* **2009**, *16*, 3775−3796.
(6) Ollis, W. D.; Ramsy, M. V. J.; Sutherland, I. O.; Mongkolsuk, S. The constitution of gambogic acid. *Tetrahedron* **1965**, *21*, 1453−1470.
(7) Ren, Y.; Yuan, C.; Chai, H. B.; Ding, Y.; Li, X. C.; Ferreira, D.; Kinghorn, A. D. Absolute configuration of (−)-gambogic acid, and antitumor agent. *J. Nat. Prod.* **2011**, *74*, 460−463.
(8) Asano, J.; Chiba, K.; Tada, M.; Yoshii, T. Cytotoxic xanthones from *Garcinia hanburyi*. *Phytochemistry* **1996**, *41*, 815−820.
(9) Han, Q. B.; Wang, Y. L.; Yang, L.; Tso, T. F.; Qiao, C. F.; Song, J. Z.; Xu, L. J.; Chen, S. L.; Yang, D. J.; Xu, H. X. Cytotoxic polyprenylated xanthones from the resin of *Garcinia hanburyi*. *Chem. Pharm. Bull.* **2006**, *54*, 265−267.
(10) Cao, S. G.; Sng, V. H. L.; Wu, X. H.; Sim, K. Y.; Tan, B. H. K.; Pereira, J. T.; Goh, S. H. Novel cytotoxic polyprenylated xanthonoids from *Garcinia gaudichaudii* (Guttiferae). *Tetrahedron* **1998**, *54*, 10915−10924.
(11) Thoisen, O.; Fahy, J.; Dumontet, V.; Chiaroni, A.; Riche, C.; Tri, M. V.; Sevenet, T. Cytotoxic prenylxanthones from *Garcinia bracteata*. *J. Nat. Prod.* **2000**, *63*, 441−446.
(12) Wu, Z. Q.; Guo, Q. L.; You, Q. D.; Zhao, L.; Gu, H. Y. Gambogic acid inhibits proliferation of human lung carcinoma SPC-A1 cells in vivo and in vitro and represses telomerase activity and telomerase reverse transcriptase mRNA expression in the cells. *Biol. Pharm. Bull.* **2004**, *27*, 1769−1774.
(13) Zhang, H. Z.; Kasibhatla, S.; Wang, Y.; Herich, J.; Guastella, J.; Tseng, B.; Drewe, J.; Cai, S. X. Discovery, characterization and SAR of gambogic acid as a potent apoptosis inducer by a HTS assay. *Bioorg. Med. Chem.* **2004**, *12*, 309−317.
(14) Yang, Y.; Yang, L.; You, Q. D.; Nie, F. F.; Gu, H. Y.; Zhao, L.; Wang, X. T.; Guo, Q. L. Differential apoptotic induction of gambogic acid, a novel anticancer natural product, on hepatoma cells and normal hepatocytes. *Cancer Lett.* **2007**, *256*, 259−266.
(15) Zhao, L.; Zhen, C.; Wu, Z.; Hu, R.; Zhou, C.; Guo, Q. General pharmacological properties, developmental toxicity, and analgesic activity of gambogic acid, a novel natural anticancer agent. *Drug Chem. Toxicol.* **2010**, *33*, 88−96.
(16) Gu, H.; Wang, X.; Rao, S.; Wang, J.; Zhao, J.; Ren, F. L.; Mu, R.; Yang, Y.; Qi, Q.; Liu, W.; Lu, N.; Ling, H.; You, Q.; Guo, Q. Gambogic acid mediates apoptosis as a p53 inducer through down-regulation of mdm2 in wild-type p53-expressing cancer cells. *Mol. Cancer Ther.* **2008**, *7*, 3298−3305.
(17) Huang, H.; Chen, D.; Li, S.; Li, X.; Liu, N.; Lu, X.; Liu, S.; Zhao, K.; Zhao, C.; Guo, H.; Yang, C.; Zhou, P.; Dong, X.; Zhang, C. Guanmei; Dou, Q. P.; Liu, J. Gambogic acid enhances proteasome inhibitor-induced anticancer activity. *Cancer Lett.* **2011**, *301*, 221−228.
(18) Yu, J.; Guo, Q. L.; You, Q. D.; Zhao, L.; Gu, H. Y.; Yang, Y.; Zhang, H. W.; Tan, Z.; Wang, X. Gambogic acid-induced G2/M phase cell-cycle arrest via disturbing CDK7-mediated phosphorylation of CDC2/p34 in human gastric carcinoma BGC-823 cells. *Carcinogenesis* **2007**, *28*, 632−638.
(19) Qiang, L.; Yang, Y.; You, Q. D.; Ma, Y. J.; Yang, L.; Nie, F. F.; Gu, H. Y.; Zhao, L.; Lu, N.; Qi, Q.; Liu, W.; Wang, X. T.; Guo, Q. L. Inhibition of glioblastoma growth and angiogenesis by gambogic acid: An in vitro and in vivo study. *Biochem. Pharmacol.* **2008**, *75*, 1083−1092.
(20) Yi, T.; Yi, Z.; Cho, S. K.; Luo, J.; Pandey, M. K.; Aggarwal, B. B.; Liu, M. Gambogic acid inhibits angiogenesis and prostate tumor

growth by suppressing vascular endothelial growth factor receptor 2 signaling. *Cancer Res.* **2008**, *68*, 1843−1850.
(21) Li, C.; Lu, N.; Qi, Q.; Li, F.; Ling, Y.; Chen, Y.; Qin, Y.; Li, Z.; Zhang, H.; You, Q.; Guo, Q. Gambogic acid inhibits tumor cell adhesion by suppressing integrin β1 and membrane lipid rafts-associated integrin signaling pathway. *Biochem. Pharmacol.* **2011**, *82*, 1873−1883.
(22) Zhai, D.; Jin, C.; Shiau, C. W.; Kitada, S.; Satterthwait, A. C.; Reed, J. C. Gambogic acid is an antagonist of antiapoptotic Bcl-2 family proteins. *Mol. Cancer Ther.* **2008**, *7*, 1639−1646.
(23) Yang, J.; Li, C.; Ding, L.; Guo, Q.; You, Q.; Jin, S. Gambogic acid deactivates cytosolic and mitochondrial thioredoxins by covalent binding to the functional domain. *J. Nat. Prod.* **2012**, *75*, 1108−1116.
(24) Qin, Y.; Meng, L.; Hu, C.; Duan, W.; Zuo, Z.; Lin, L.; Zhang, X.; Ding, J. Gambogic acid inhibits the catalytic activity of human topoisomerase IIalpha by binding to its ATPase domain. *Mol. Cancer Ther.* **2007**, *6*, 2429−2440.
(25) Wang, T.; Wei, J.; Qian, X.; Ding, Y.; Yu, L.; Liu, B. Gambogic acid, a potent inhibitor of survivin, reverses docetaxel resistance in gastric cancer cells. *Cancer Lett.* **2008**, *262*, 214−222.
(26) Kasibhatla, S.; Jessen, K. A.; Maliartchouk, S.; Wang, J. Y.; English, N. M.; Drewe, J.; Qiu, L.; Archer, S. P.; Ponce, A. E.; Sirisoma, N.; Jiang, S.; Zhang, H. Z.; Gehlsen, K. R.; Cai, S. X.; Green, D. R.; Tseng, B. A role for transferrin receptor in triggering apoptosis when targeted with gambogic acid. *Proc. Natl. Acad. Sci. U S A* **2005**, *102*, 12095−12100.
(27) Pandey, M. K.; Sung, B.; Ahn, K. S.; Kunnumakkara, A. B.; Chaturvedi, M. M.; Aggarwal, B. B. Gambogic acid, a novel ligand for transferring receptor, potentiates TNF-induced apoptosis through modulation of the nuclear factor-κB signaling pathway. *Blood* **2007**, *110*, 3517−3525.
(28) Davenport, J.; Manjarrez, J. R.; Peterson, L.; Krumm, B.; Blagg, B. S.; Matts, R. L. Gambogic acid, a natural product inhibitor of Hsp90. *J. Nat. Prod.* **2011**, *74*, 1085−1092.
(29) Wang, X.; Chen, Y.; Han, Q. B.; Chan, C. Y.; Wang, H.; Liu, Z.; Cheng, C. H.; Yew, D. T.; Lin, M. C.; He, M. L.; Xu, H. X.; Sung, J. J.; Kung, H. F. Proteomic identification of molecular targets of gambogic acid: Role of stathmin in hepatocellular carcinoma. *Proteomics* **2009**, *9*, 242−253.
(30) Palempalli, U. D.; Gandhi, U.; Kalantari, P.; Vunta, H.; Arner, R. J.; Narayan, V.; Ravindran, A.; Prabhu, K. S. Gambogic acid covalently modifies IkappaB kinase-beta subunit to mediate suppression of lipopolysaccharide-induced activation of NF-kappaB in macrophages. *Biochem. J.* **2009**, *419*, 401−409.
(31) Sun, H.; Chen, F.; Wang, X.; Liu, Z.; Yang, Q.; Zhang, X.; Zhu, J.; Qiang, L.; Guo, Q.; You, Q. Studies on chemical modification and biology of a natural product, Gambogic acid (IV): Identification of IκB Kinase-beta (IKKβ) as the molecular target and determination of the pharmacophoric scaffold. *Eur. J. Med. Chem.* **2012**, *51*, 110−123.
(32) Wang, J.; Zhaoaaa, Li.; Hu, Y.; Guo, Q.; Zhang, L.; Wang, X.; Li, N.; You, Q. Studies on chemical modification and biology of a natural product, gambogic acid (I): Synthesis and biological evaluation of oxidized analogues of gambogic acid. *Eur. J. Med. Chem.* **2009**, *44*, 2611−2620.
(33) Chantarasriwong, O.; Batova, A.; Chavasiri, W.; Theodorakis, E. A. Chemistry and biology of the caged *Garcinia* xanthones. *Chem.—Eur. J.* **2010**, *16*, 9944−9962.
(34) He, L.; Ling, Y.; Fu, L.; Yin, D.; Wang, X.; Zhang, Y. Synthesis and biological evaluation of novel derivatives of gambogic acid as anti-hepatocellualar carcinoma agents. *Bioorg. Med. Chem.* **2012**, *22*, 289−292.
(35) Batova, A.; Lam, T.; Waschol owski, V.; Yu, A. L.; Giannis, A.; Theodorakis, E. A. Synthesis and evaluation of caged *Garcinia* xanthones. *Org. Biomol. Chem.* **2007**, *5*, 494−500.
(36) Zhang, X.; Li, X.; Sun, H.; Jiang, Z.; Tao, L.; Gao, Y.; Guo, Q.; You, Q. Synthesis and evaluation of novel aza-caged *Garcinia* xanthones. *Org. Biomol. Chem.* **2012**, *10*, 3288−3299.
(37) Chantarasriwong, O.; Cho, W. C.; Batova, A.; Chavasiri, W.; Moore, C.; Rheingold, A. L.; Theodorakis, E. A. Evaluation of the pharmacophoric motif of the caged *Garcinia* xanthones. *Org. Biomol. Chem.* **2009**, *5*, 4886−4894.
(38) Wang, X.; Lu, N.; Yang, Q.; Gong, D.; Lin, C.; Zhang, S.; Xi, M.; Gao, Y.; Wei, L.; Guo, Q.; You, Q. Studies on chemical modification and biology of a natural product, gambogic acid (III): Determination of the essential pharmacophore for biological activity. *Eur. J. Med. Chem.* **2011**, *46*, 1280−1290.
(39) Kuemmerle, J.; Jiang, S.; Tseng, B.; Kasibhatla, S.; Drewe, J.; Cai, S. X. Synthesis of caged 2,3,3a,7a-terahydro-3,6-methanobenzofuran-7(6*H*)-ones: Evaluating the minimum structure for apoptosis induction by gambogic acid. *Bioorg. Med. Chem.* **2008**, *16*, 4233−4241.
(40) Wang, J.; Ma, J.; You, Q.; Zhao, L.; Wang, F.; Li, C.; Guo, Q. Studies on chemical modification and biology of a natural product, gambogic acid (II): Synthesis and bioevaluation of gambogellic acid and its derivatives. *Eur. J. Med. Chem.* **2010**, *45*, 4343−4353.
(41) Wang, X.; Lu, N.; Yang, Q.; Dai, Q.; Tao, L.; Guo, X.; Guo, Q.; You, Q. Spectacular modification of gambogic acid on microwave irradiation in methanol: Isolation and structure identification of two products with potent anti-tumor activity. *Bioorg. Med. Chem.* **2010**, *20*, 2438−2442.
(42) Li, X.; Zhang, X.; Sun, H.; Zhang, L.; Gao, Y.; Wang, J.; Guo, Q.; You, Q. Synthesis and anti-tumor evaluation of novel C-37 modified derivatives of gambogic acid. *Chin. J. Chem.* **2012**, *30*, 1083−1091.
(43) Sun, H.-P.; Liu, Z.-L.; Xue, X.; Gao, Y.; Zhang, L.; Guo, Q.-L.; You, Q.-D. Studies on chemical structure modification and structure−activity relationship of derivatives of gambogic acid at C(39). *Chem. Biodiv.* **2012**, *9*, 1579−1590.
(44) Zhang, X.-J; Li, X.; Yang, Y.-R.; Sun, H.-P.; Gao, Y.; Zhang, L.; Wang, J.-X.; Guo, Q.-L.; You, Q.-D. Studies on chemical structure modification and structure−activity relationship of derivatives of gambogic acid at C(34). *Chem. Biodiv.* **2012**, *9*, 2295−2308.
(45) Nicolaou, K. C.; Li, J. "Biomimetic" cascade reactions in organic synthesis: Construction of 4-oxatricyclo[4.3.1.0]decan-2-one systems and total synthesis of 1-*O*-methylforbesione via tandem Claisen rearrangement/Diels−Alder reaction. *Angew. Chem., Int. Ed.* **2001**, *40*, 4264−4268.
(46) Tisdale, E. J.; Li, H.; Vong, B. G.; Kim, S. H.; Theodorakis, E. A. Regioselective synthesis of the tricyclic core of lateriflorone. *Org. Lett.* **2003**, *5*, 1491−1494.
(47) Nicolaou, K. C.; Sasmal, P. K.; Xu, H. Biomimetically inspired total synthesis and structure activity relationships of 1-*O*-methyllateriflorone. 6π Electrocyclizations in organic synthesis. *J. Am. Chem. Soc.* **2004**, *126*, 5493−5501.
(48) Tisdale, E. J.; Slobodov, I.; Theodorakis, E. A. Unified synthesis of caged *Garcinia* natural products based on a site-selective Claisen/Diels−Alder/Claisen rearrangement. *Proc. Natl. Acad. Sci. U. S. A.* **2004**, *101*, 12030−12035.
(49) Li, N.-G.; Wang, J.-X.; Liu, X.-R.; Lin, C.-J.; You, Q.-D.; Guo, Q.-L. A novel and efficient route to the construction of the 4-oxatricyclo[4.3.1.0]decan-2-one scaffold. *Tetrahedron Lett.* **2007**, *48*, 6586−6589.
(50) Liu, Z.-L.; Wang, X.-J.; Li, N.-G.; Sun, H.-P.; Wang, J.-X.; You, Q.-D. Total synthesis of aldehyde-containing *Garcinia* natural products isomorellin and gaudichaudione A. *Tetrahedron* **2011**, *67*, 4774−4779.
(51) Li, X.; Zhang, X.; Yu, Z.; Liu, X.; You, Q.; Guo, Q. Microwave-assisted Claisen rearrangement/Diels−Alder cascade reaction for the synthesis of caged *Garcinia* natural products and analogues. *J. Chem. Res.* **2012**, *35*, 630−633.
(52) Avdeef, A.; Tsinman, O. Miniaturized rotating disk intrinsic dissolution rate measurement: Effect of buffer capacity in comparisons to traditional Wood's apparatus. *Pharm. Res.* **2008**, *25*, 2613−2627.
(53) Avdeef, A.; Bucher, J. J. Accurate measurements of the concentration of hydrogen ions with a glass electrode: Calibrations using the Prideaux and other universal buffer solutions and a computer-controlled automatic titrator. *Anal. Chem.* **1987**, *50*, 2137−2142.
(54) Egan, W. J.; Merz, K. M.; Baldwin, J. J. Prediction of drug absorption using multivariate statistics. *J. Med. Chem.* **2000**, *43*, 3867−3877.

(55) Egan, W. J.; Lauri, G. Prediction of intestinal permeability. *Adv. Drug Delivery Rev.* **2002**, *54*, 273−289.
(56) Kelder, J.; Grootenhuis, P. D.; Bayada, D. M.; Delbressine, L. P.; Ploemen, J.-P. Polar molecular surface as a dominating determinant for oral absorption and brain penetration of drugs. *Pharm. Res.* **1999**, *16*, 1514−1519.
(57) Hollingshead, M. G. Antitumor efficacy testing in rodents. *J. Nat. Cancer Inst.* **2008**, *100*, 1500−1510.